

N O T I C E

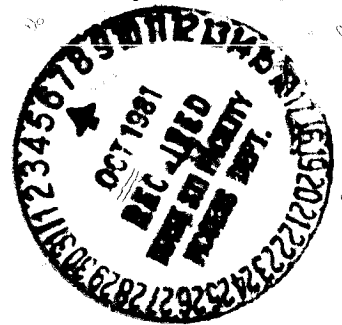
THIS DOCUMENT HAS BEEN REPRODUCED FROM
MICROFICHE. ALTHOUGH IT IS RECOGNIZED THAT
CERTAIN PORTIONS ARE ILLEGIBLE, IT IS BEING RELEASED
IN THE INTEREST OF MAKING AVAILABLE AS MUCH
INFORMATION AS POSSIBLE

881-32382

63/55

UNCLAS
27481

POWER TRANSISTOR COMPANY
800 WEST CARSON STREET
TORRANCE, CA 90502



PREPARED FOR
NATIONAL AERONAUTICS AND SPACE ADMINISTRATION
NASA LEWIS RESEARCH CENTER
CONTRACT NAS3-22539

DEVELOPMENT & FABRICATION
OF A
FAST RECOVERY, HIGH VOLTAGE POWER DIODE

POWER TRANSISTOR COMPANY
800 WEST CARSON STREET
TORRANCE, CA 90502

PREPARED FOR
NATIONAL AERONAUTICS AND SPACE ADMINISTRATION
NASA LEWIS RESEARCH CENTER
CONTRACT NAS3-22539

1 Report No CR-165411	2 Government Accession No	3 Recipient's Catalog No	
4 Title and Subtitle Development and Fabrication of a Fast Recovery, High Voltage Power Diode		5 Report Date June 1981	
		6 Performing Organization Code	
7 Author(s) A. H. Berman, V. Balodis, J. J. Cuffin, C. Gaugh, H. H. Karatnicki		8 Performing Organization Report No	
		10 Work Unit No	
9 Performing Organization Name and Address Power Transistor Company 800 West Carson Street Torrance, CA 90502		11 Contract or Grant No NAS3-22539	
		13 Type of Report and Period Covered Contractor Report Final	
12 Sponsoring Agency Name and Address National Aeronautics & Space Administration Lewis Research Center Cleveland, OH 44135		14 Sponsoring Agency Code	
15 Supplementary Notes Project Manager, Gale Sundberg, Space Propulsion and Power Division NASA Lewis Research Center, Cleveland, Ohio			
16 Abstract A high voltage, high current, fast recovery silicon diode has been designed and fabricated utilizing a positive bevel PIN mesa structure with glass passivation. The diodes are encapsulated in a standard DO-5 package and have the following characteristics: peak inverse voltage, 1200 volts - forward voltages at 50 amperes, 1.5 volts - reverse recovery time of 200 nanoseconds. This project describes the use of positive bevels for PIN mesa structures to achieve high voltages. The technique of glass passivation for mesa structures is described. The utilization of high-energy radiation to control the lifetime of carriers in silicon is reported as a means to achieve fast recovery times. Characterization data is reported and is in agreement with design concepts developed for power diodes.			
17 Key Words (Suggested by Author(s)) Power Diodes Glass Passivation Reverse Recovery Time Positive Beveling Electron Radiation Neutron Transmutation		18 Distribution Statement Unclassified-Unlimited	
19 Security Classif (of this report) Unclassified	20 Security Classif (of this page) Unclassified	21 No of Pages	22 Price*

* For sale by the National Technical Information Service Springfield VA 22161

TABLE OF CONTENTS

	<u>Page</u>
List of Figures	iii
List of Tables	v
List of Drawings	vi
1. Summary	1
2. Introduction	2
3. Device Design	4
3.1 Structure	4
3.2 Voltage Design	7
3.3 Reverse Recovery Time	18
3.4 Forward Voltage Drop	23
3.5 Trade-offs	29
4. Wafer Processing	30
4.1 Diffusion and Lap & Polish	30
4.2 Positive Bevel Moat	30
4.3 Glass Passivation	31
4.4 Metallization	31
4.5 Wafer Test and Dicing	32
5. Encapsulation	34
5.1 Package	34
5.2 Assembly	34
5.3 Polarity Trade-offs	37
5.4 High Voltage Cap	41
5.5 Thermal Ratings	42
6. Test	44
6.1 Test Plan	44
6.2 Non-Repetitive Peak Surge Currents, I_{FSM}	45
6.3 Reverse Recovery Time, t_{rr}	46
6.4 Forward Voltage, V_{FM}	54
6.5 DC Blocking Voltage, V_R	54
6.6 Reverse Current, I_R	54
7. Electrical Performance	56
7.1 Characteristic Curves	56

	<u>Page</u>
8. Conclusion	74
9. Acknowledgements	76
10. References	77
11. Appendix	78
11.1 Specifications for Fast Recovery, High Voltage Power Diode	78

LIST OF FIGURES

	<u>Page</u>
Figure 1 Diode surface geometry	6
Figure 2 Ionization constants	8
Figure 3 Breakdown voltage curves	11
Figure 4 Depletion layer thickness curves	12
Figure 5 Depletion layer diagram	13
Figure 6 $P^+-N_1-N^+$ junction with a positive bevel	14
Figure 7 Planar structure junction	15
Figure 8 Charge density profile	16
Figure 9 Electric field diagram I	16
Figure 10 Electric field diagram II	17
Figure 11 Reverse recovery time	18
Figure 12 Forward voltage drop	24
Figure 13 Intrinsic region	26
Figure 14 Process sequence outline	33
Figure 15 Solder reflow assembly, reverse polarity diode	36
Figure 16 Solder reflow assembly, initial proposal	38
Figure 17 Close-up cross section of Figure 16	39
Figure 18 Normal polarity assembly, modified version	40
Figure 19 Thermal resistance, equivalent diagram	43
Figure 20 Test circuit block diagram	45
Figure 21 Diode testing fixture	47
Figure 22 Peak surge current pulse	48
Figure 23 Reverse recovery waveform	50
Figure 24 Typical t_{rr} waveforms	51

	<u>Page</u>
Figure 25 Forward voltage, V_{FM}	55
Figure 26 Device #031-Forward characteristic curve	58
Figure 27 Device #038-Forward characteristic curve	59
Figure 28 Device #039-Forward characteristic curve	60
Figure 29 Device #046-Forward characteristic curve	61
Figure 30 Device #060-Forward characteristic curve	62
Figure 31 Device #031-Reverse leakage	63
Figure 32 Device #038-Reverse leakage	64
Figure 33 Device #039-Reverse leakage	65
Figure 34 Device #046-Reverse leakage	66
Figure 35 Device #060-Reverse leakage	67
Figure 36 Leakage versus temperature	68
Figure 37 Device #031-Capacitance versus reverse voltage	69
Figure 38 Device #038-Capacitance versus reverse voltage	70
Figure 39 Device #039-Capacitance versus reverse voltage	71
Figure 40 Device #046-Capacitance versus reverse voltage	72
Figure 41 Device #060-Capacitance versus reverse voltage	73

LIST OF TABLES

	<u>Page</u>
Table 1 V_{BP} versus intrinsic thickness	10
Table 2 Forward voltage drop, blocking voltage and reverse recovery time of lot NASA-007 devices radiated with 12 megarads β radiation (after packaging)	21
Table 3 Forward voltage drop, blocking voltage and reverse recovery time of lot NASA-007 devices radiated with 16 megarads β radiation (after packaging)	22
Table 4 Delivered diode test data	52

DRAWINGS

1. D0-5 stud - IMPEX, 1404
2. D0-5 cap - 50-0016
3. Moly tab, cathode - 50-0003-4
4. Moly tab, anode - 50-0003-3
5. Internal lead - 50-0011
6. Solder preform, cathode - 50-0004-7
7. Solder preform, anode - 50-0004-6
8. Fixture, soldering - 50-0010
9. Stud base - Nipert Co. P/N 068-8903
10. D0-5 rock top - 50-0017

1. SUMMARY

The objective of this program is to develop a fast recovery 1200 volt, 50 ampere, silicon diode as specified by NASA Contract Number NAS3-22539, dated September 18, 1980.

In order to meet the specifications of this contract a PIN diffused structure was proposed. A positive bevel mesa structure was used to reduce surface fields in order to utilize a lower starting silicon resistivity in order to achieve the specified forward voltage with a minimum silicon area.

A positive bevel was etched into the p-n junction, which was later glass passivated.

Metallization used for contacting the cathode and anode areas was a TRI-METAL composition, which permitted solder reflow assembly.

The device was encapsulated in a DO-5 diode package. Solder-reflow techniques were used to assemble the device. The characterization data presented is in agreement with the design concepts presented in this report.

All devices delivered to NASA under this contract met or exceeded the required specifications. A full characterization of the diode is included in this final report.

2. INTRODUCTION

The NASA requirement in avionic systems for electrical power beyond the ten kilowatt level requires the use of a fast switching, high voltage, high current transistor.

The use of a fast switch, high voltage, high current power transistor necessitates a fast switching, high voltage diode with equivalent power capability of the transistor.

The recovery time of the diode would have to be shorter than that of the transistor by a factor of two in order to protect the transistor.

Diodes with these characteristics are used in snubber networks, as freewheeling diodes in inverter circuits and as rectifiers in high frequency power conversion equipment.

The combination of fast switch speed and high voltage required by the NASA specification is in the realm of the state-of-the-art of power semiconductor device fabrication.

The NASA requirement for such a high voltage, fast switching diode is also a requirement for the industrial electronics market.

Specific applications are in electric vehicle motor drives, AC and DC motor controllers. The 1000 volt capability of the diode will have an application in industrial motor controllers where the bus line

voltages are 480 volts. At the present time, two fast switch low voltage parts must be used in series to achieve the 1000 volt requirement and speed requirement at the expense of switching efficiency.

Diodes fabricated under this contract have been utilized in AC motor controller inverter circuits operating from 480 volt lines.

3. DEVICE DESIGN

3.1 Structure

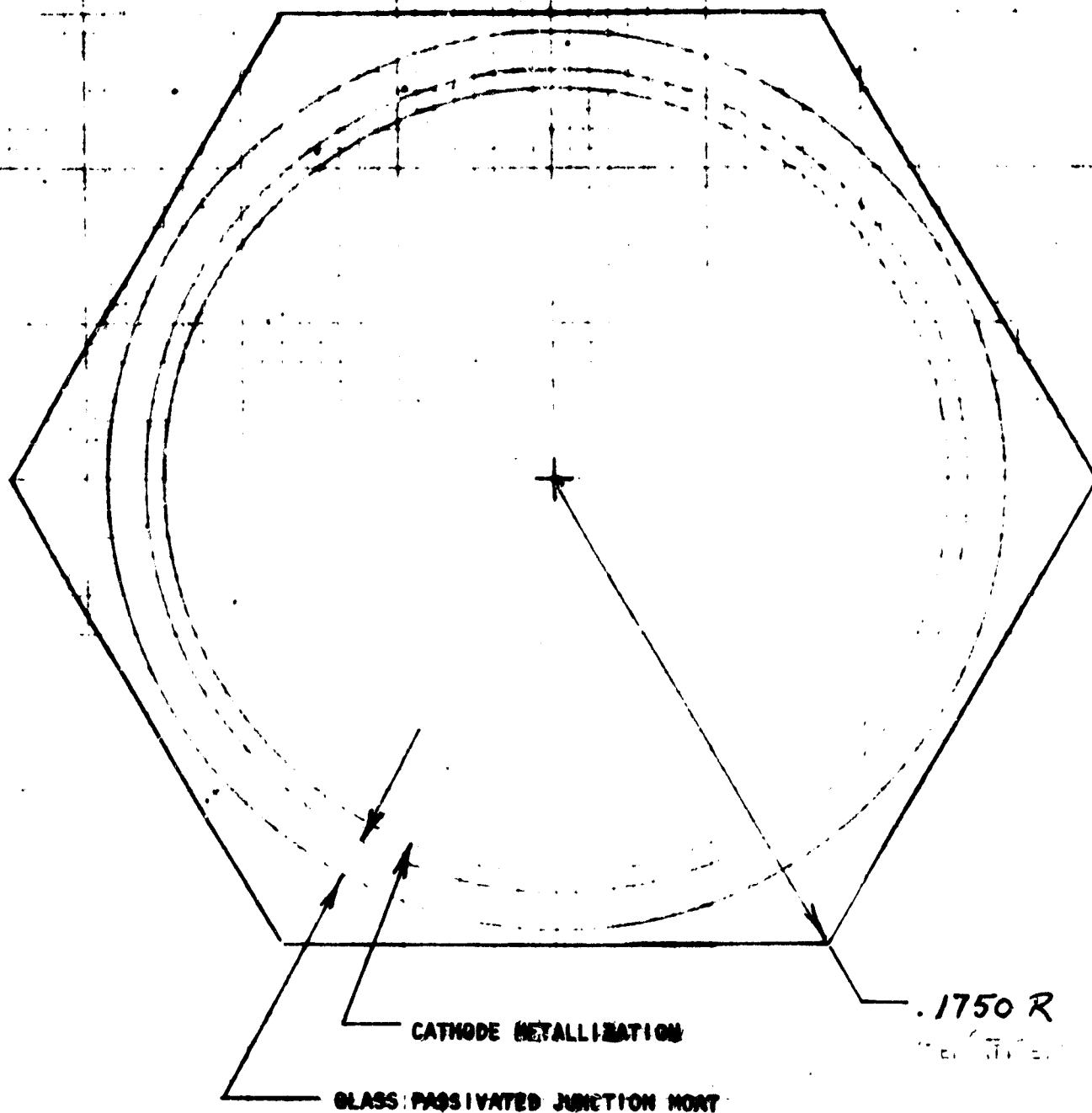
The device is fabricated from 35 Ωcm thermal neutron, transmutation N-type doped, float zone silicon. Float zone silicon exhibits high minority carrier lifetime and low oxygen and carbon content. Neutron transmutation doping involves the nuclear conversion of silicon atoms into phosphorus dopant atoms by exposing (intrinsic) silicon to a flux of thermal neutrons in a nuclear reactor core. The nuclear reaction is $\text{Si}_{14}^{30} + n \rightarrow \text{P}_{15}^{31} + e^-$. The silicon isotope Si_{14}^{30} absorbs a thermal neutron and becomes Si_{14}^{31} , Si_{14}^{31} is unstable and emits an electron to become P_{15}^{31} . This technique allows the fabrication of N-doped float zone silicon of extreme homogeneity, i.e., small radial variations and reduced striations (resistivity microvariations); a result impossible by any of the other growing and doping methods. Low resistivity variations across the wafer minimizes the wafer thickness required as a function of the resistivity and the intrinsic layer minority carrier lifetime.

Terminating the p-n junction with a glass passivated positive bevel moat allows the use of material with a relatively low resistivity level. The use of this material improves the trade-offs between blocking voltage, forward voltage drop and switch time.

The basic impurity concentration profile consists of a deep diffused P^+ anode 125 to 140 microns deep, an intrinsic material layer and a shallow (15 microns), low resistivity N^+ cathode cap. The diffused anode and low resistivity cathode aid in reducing the diode's double injection forward bias voltage drop. The thick intrinsic layer is required to sustain high voltage reverse biases.

A hexagonal geometry is employed in order to reduce the forward voltage drop by reducing the current density. This geometry maximizes the use of the circular area of the D0-5 package while allowing the wafer to be diced easily and by conventional means. See Figure 1.

DIODE SURFACE SECTION



ORIGINAL PAGE IS
OF POOR QUALITY

FIGURE 1

3.2 Voltage Design

The requirement that the device endure a peak non-repetitive reverse voltage of 1.25 times the blocking voltage of 1000 volts or 1250 volts without undergoing bulk breakdown will be met by using 35 ohm-cm starting (intrinsic) material. Figure 2, taken from Reference 1, indicates 35 ohm-cm silicon, with a donor concentration of 1.5×10^{14} atoms/cc, will allow a reverse voltage of between 1600 and 1700 volts when the junction is 140 microns deep, which is the case with this device.

For a diffused (graded) junction, the required depletion region thickness is given by the following formula:

$$(1) \quad d = (12 K \epsilon_0 V_{BD} / qa)^{1/3}$$

where

a = the grade constant of a diffused junction

$$= \frac{N_D}{X_J} \ln \left(\frac{P_O}{N_D} \right) = 12.88 / \mu^4$$

X_J = the junction depth = 140 microns

P_O = the diffused surface concentration = 2.5×10^{19} atoms/cc

d = total depletion layer thickness

ϵ_0 = permittivity of free space = $55.4 \frac{\text{electron charges}}{\text{volt-micron}}$

K = dielectric constant of silicon = 12

q = electron charge = 1.6×10^{19} coulombs

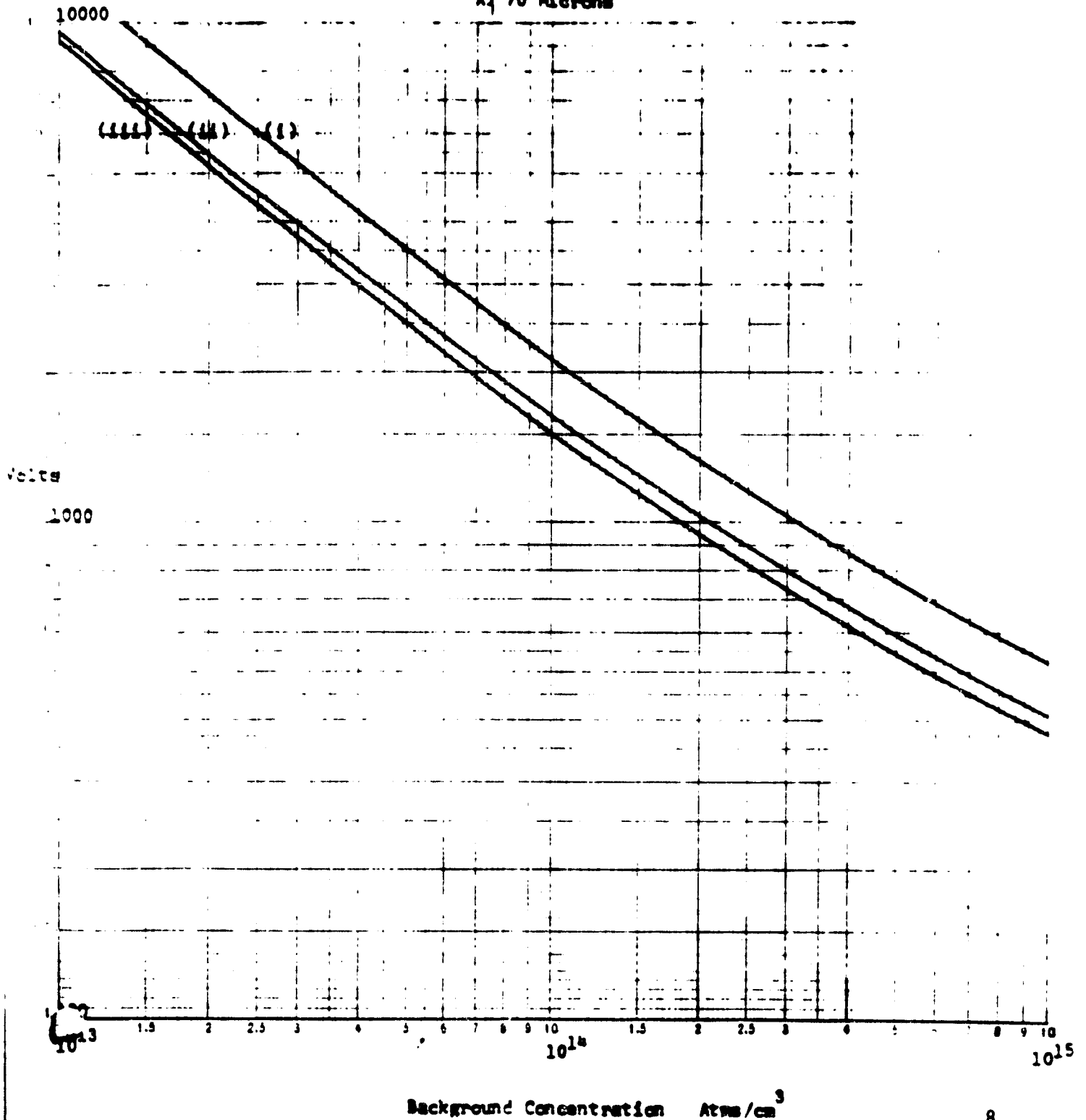
N_D = density of donor atoms in 35 ohm-cm N-type silicon
= 1.5×10^{14} atoms/cc

and V_{BD} = the breakdown voltage = 1250 volts

IONIZATION CONSTANTS

- (i) Meserlian
- (ii) Roll & Van Overstraeten
- (iii) Lee et al

FIGURE 2
Avalanche Breakdown
Surface Concentration 10^{19}
 X_1 70 Microns



The calculation of the depletion layer yields a thickness of 92 microns. The region depleted of carriers lies partly in the P⁺ layer and partly in the intrinsic layer.

Our initial estimate of 106 microns was found from the expression for the required width of a step (non-graded) junction:

$$(2) \quad d = (2K\epsilon_0 V_{BD} / qN_D)^{1/2}$$

This provided a good estimate, later revised as data (Table 1) indicated that this width was too large.

Table 1
V_{BD} Versus Intrinsic Thickness

Lot No.	Intrinsic Thickness (microns)	V _{BD} (volts)
001	43 - 56	1000
002	56 - 58	1100
006	74 - 86	1140
007	74 - 86	1090
008	76 - 81	1175
009	81 - 89	1290

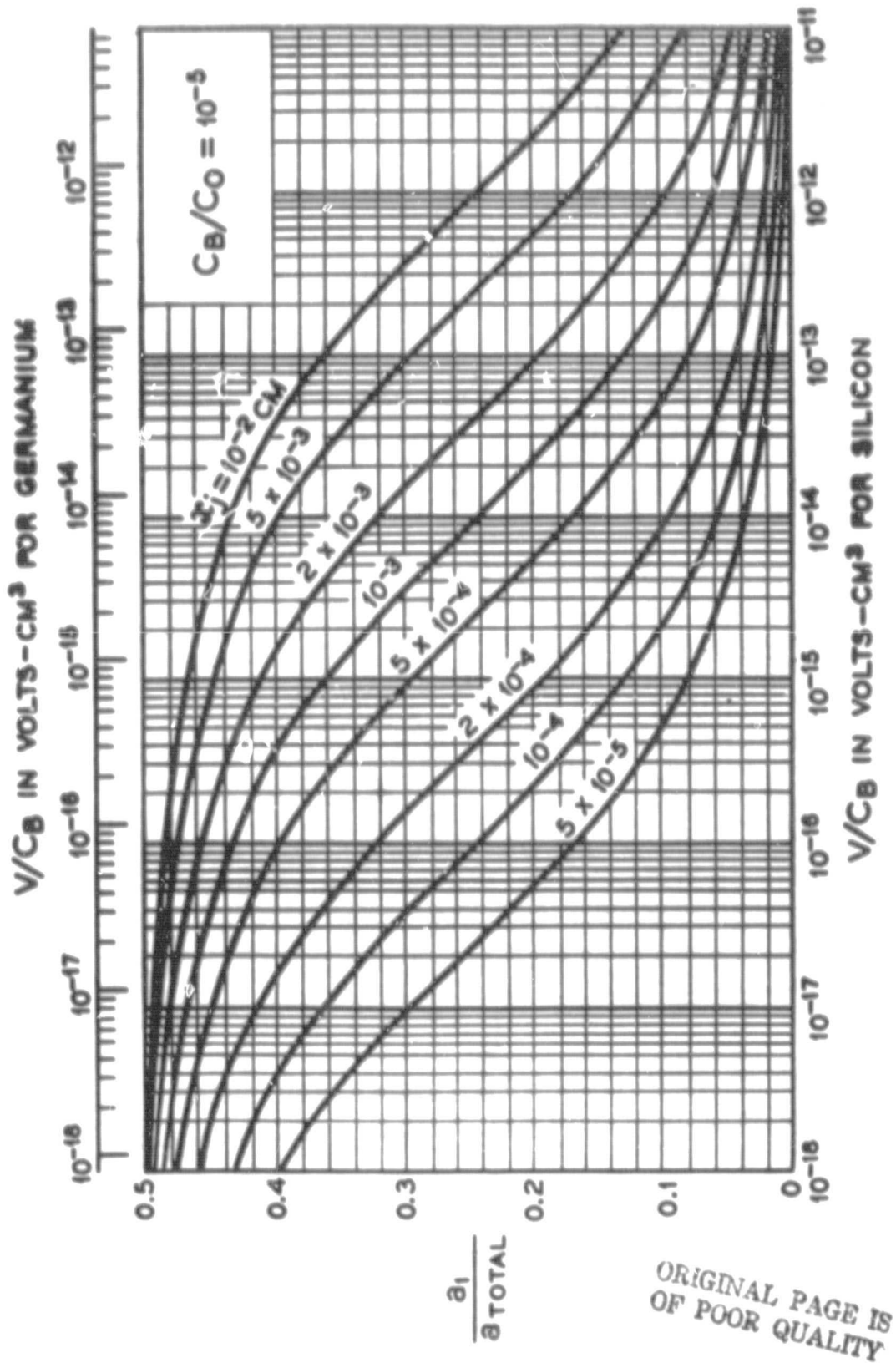


Figure 3 Breakdown voltage curves

Fig. 29 — Chart for use in range 8×10^{-6} to 8×10^{-3} , gaussian distribution.

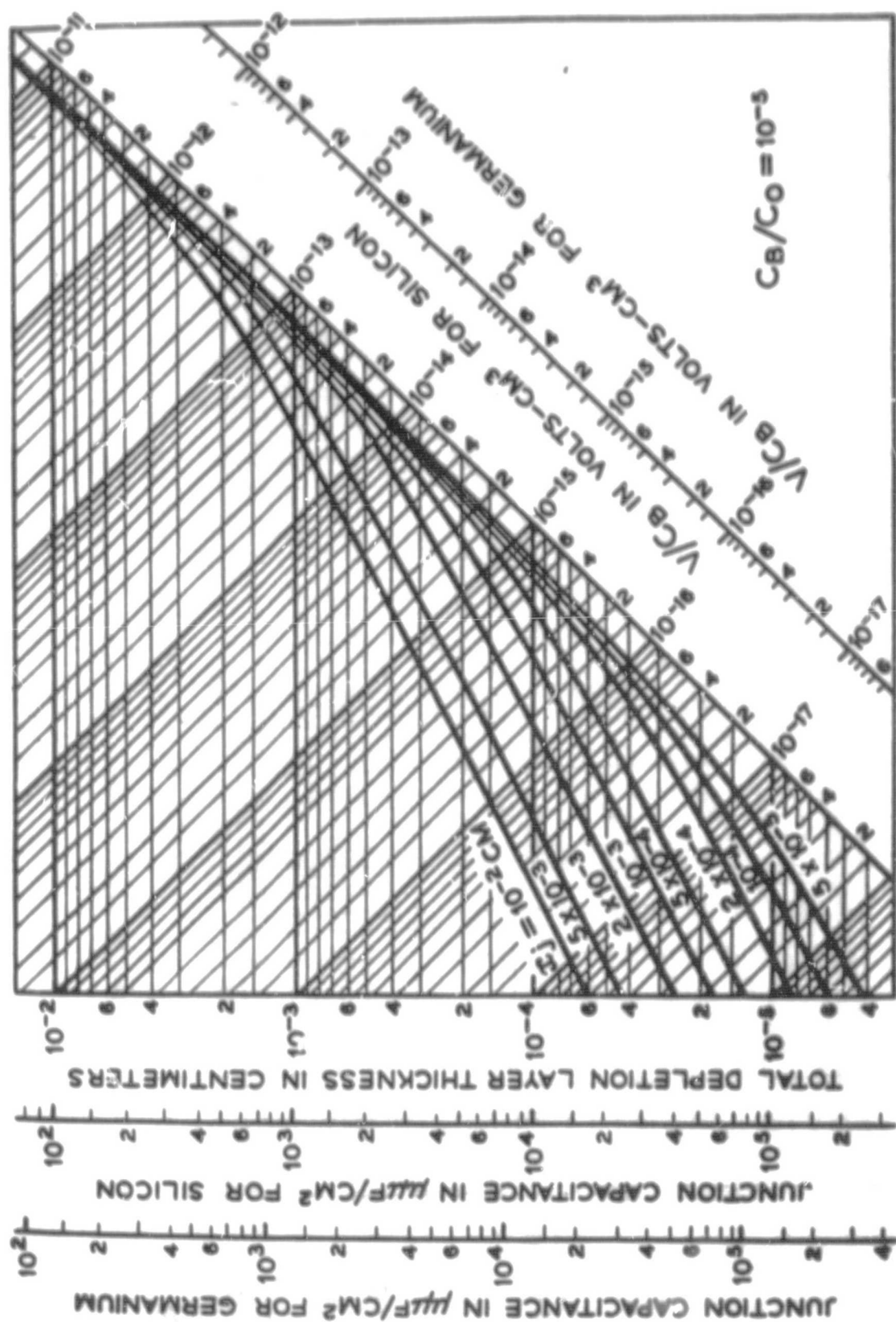


Figure 4 Depletion layer thickness curves

Fig. 21 — Chart for use in range 3×10^{-6} to 3×10^{-3} , gaussian distribution.

Figures 3 and 4, from reference 2, indicate that for a junction depth of 140 microns and surface concentration of 2.5×10^{19} atoms/cc, 15% of the depletion region lies in the P^+ layer and the intrinsic layer should be at least 85% of 92 microns or 78 microns thick to block 1250 volts.

Table 1 shows the average breakdown voltage and intrinsic layer thickness for several diffusion lots produced for this contract

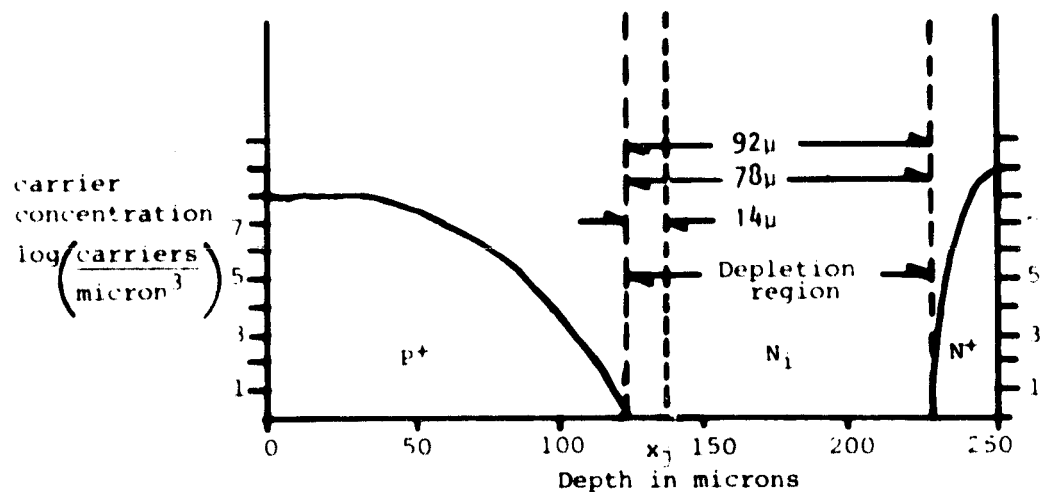
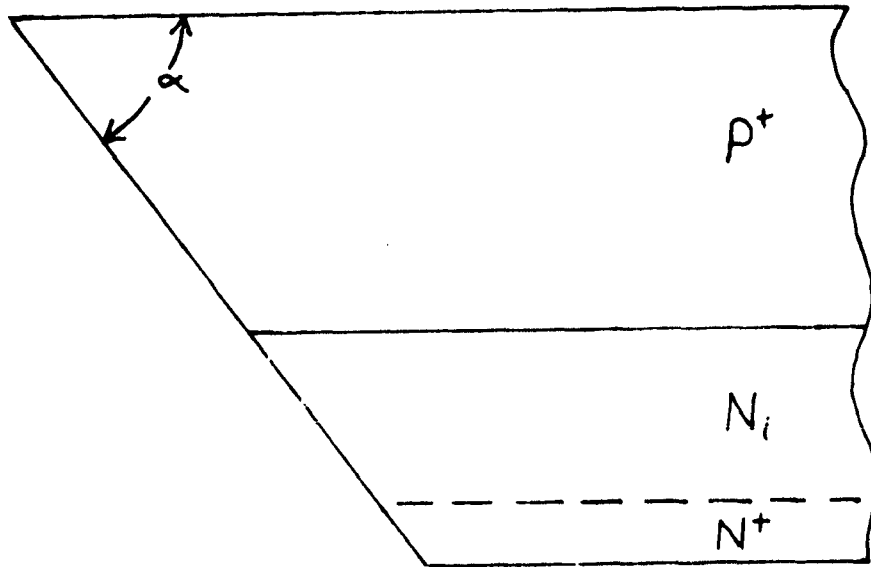


Figure 5 Depletion layer diagram

Equation (1) assumes device failure will occur due to avalanche breakdown within the bulk of the device. However, the use of a standard straight wall mesa would limit the voltage breakdown to 800 to 900 volts as the device will fail at the edge of the junction due to the higher field there. Therefore, the positive beveled mesa structure in Figure 6 is mandatory for our high voltage requirement. A planar device in Figure 7, produced by P diffusion in an N-



α = bevel angle

$P^+-N_i-N^+$ Junction with a Positive Bevel

Figure 6

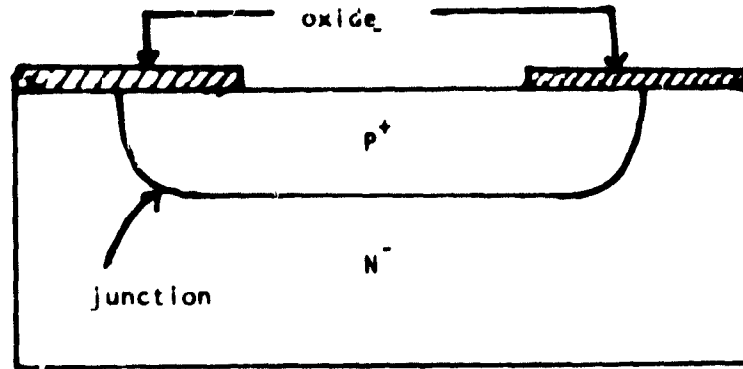


Figure 7 Planar structure junction

starting material has such concentration of the electric field (during reverse bias) at the corners that typically 30% of the blocking voltage is lost at 1000 volts. The structure in Figure 6 has a positive bevel on the edge as measured from N^- to P^+ . This is produced by groove etching from the intrinsic side. This positive bevel assures that the avalanche breakdown voltage will be the maximum allowed by the starting resistivity and diffusion profile, i.e., it will occur inside the device and not on the edge. This is shown by the following brief analysis. See Reference 3.

Avalanche breakdown occurs in a diffused junction when the applied voltage raises the internal electric field in the device to the critical field $[E_c]$, the maximum value that can be sustained in silicon (approximately 30 volts/micron) before releasing electrons from the next lowest valence level. The field arises due to carrier migration in the N and P regions towards the + and - electrodes respectively, which leaves a charged region behind to block conduction across the junction. The charged region

will follow the doping profiles away from the junction until E_c is reached.

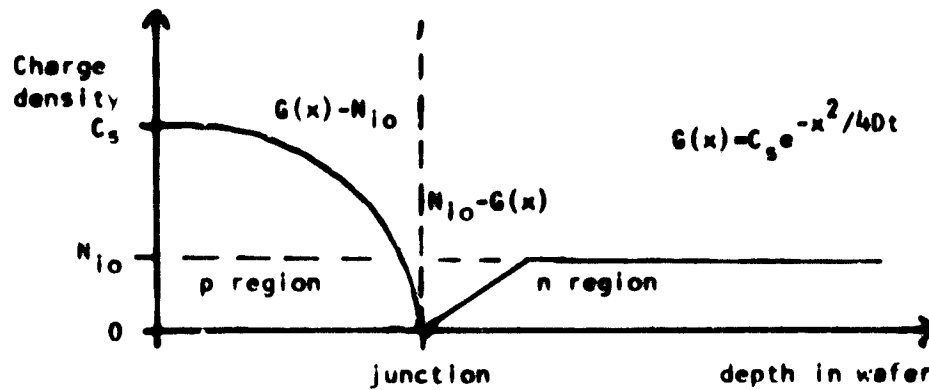


Figure 8 Charge density profile

The total charge on either side of the junction is the same, however, since the highest charge density occurs on the P side due to the steepness of the diffusion profile (Figure 8) this region will predominate at E_c . The local field is determined by integrating the charge density divided by the distance squared. See Figure 9.

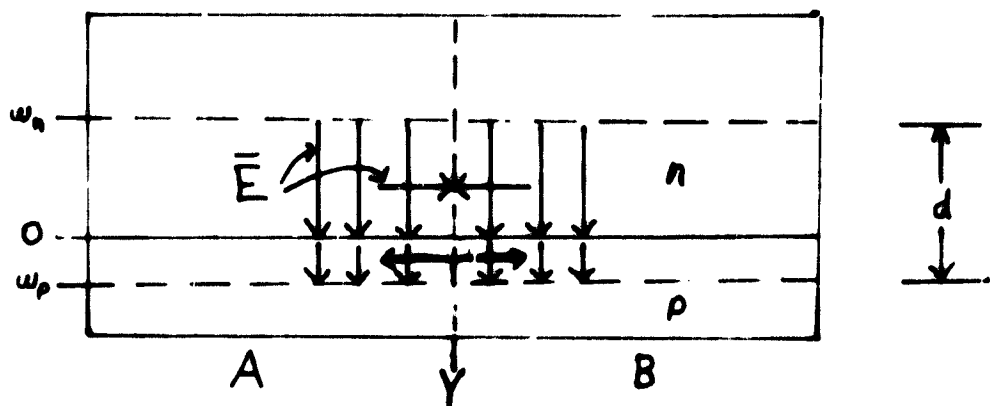


Figure 9 Electric field diagram I

Considering a point Y far from the edge, by lateral symmetry the normal field (E_n) is composed of equal contributions from both regions A and B. If the point Y is moved to the edge, or region B removed, the normal field should be half of the applied field (E_0), $E_n = E_0/2$. See Figure 10.

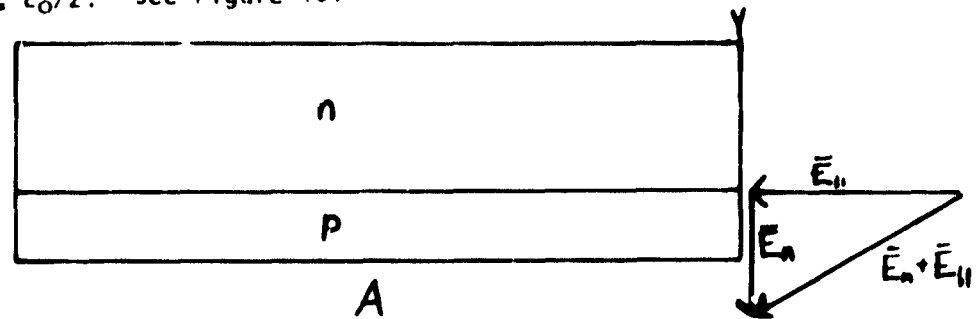


Figure 10 Electric field diagram 11

Since region B is gone, there exists a laterally unbalanced parallel field (E_{11}) at the point Y also. (We are considering only the P region since the field gradient is much higher there.) Make two assumptions for simplicity; 1) the width of the field in the P region is small compared to the depletion layer width, and 2) the charge density in the P region is uniform in both the parallel and normal directions. Then by symmetry, $E_{11} = E_0$ and $E_{11} = 2E_n$. The vector sum is in a direction 60° to the normal and of magnitude $1.1 \times E_0$. Actually, since the charged P region is not uniform, the highest field sum will exceed this value and the angle will be somewhat greater. To assure a minimum field on the edge, the bevel, or edge angle of the moat, should be 60° to the junction, i.e.,

perpendicular to the field since edge passivation material (glass) will prevent current flowing through the air.

3.3 Reverse Recovery Time

The relations between the specified rate of decay of the current, di_f/dt , the reverse recovery time, t_{rr} , and the carrier lifetime, τ , are given by solving

$$(3) \quad Q_R = \frac{1}{2}(\tau^2 di_f/dt)$$

where $Q_R = \int_0^{t_{rr}} i(t)dt$ is the recovery charge and the JEDEC test requires that $di_f/dt = 25 \times 10^6$ amps/second while t_{rr} is specified to be 200×10^{-9} seconds. See Figure 11.

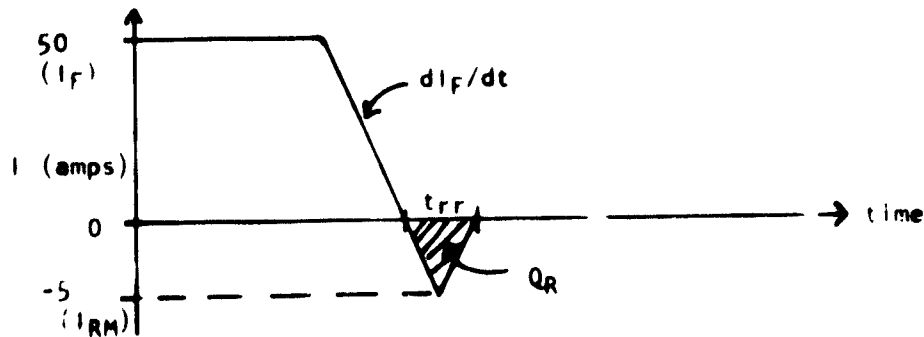


Figure 11 Reverse recovery time

$$(4) \quad Q_R = \int_0^{t_{RR}} (dIF/dt) t \, dt = \frac{(t_{RR})^2}{2} (dIF/dt) \\ = 5 \times 10^{-7} \text{ coulombs}$$

$$\text{by (3)} \quad \tau = (2Q_R/dIF/dt)^{1/2} = 2 \times 10^{-7} \text{ seconds}$$

is the required carrier lifetime.

It has been shown that high-energy radiation of silicon devices displaces silicon atoms from their normal lattice positions forming vacancies and interstitial defects. These defects act as recombination centers for electrons and holes with an energy within the forbidden range (gap) of silicon, which effect the lifetime of carriers in silicon.

The effect of electron radiation on the recombination of carriers is given by the following formula:

$$(5) \quad R = R_0 + K_T \emptyset$$

where R = the post-irradiation recombination rate, sec^{-1}

R_0 = the pre-irradiation recombination rate, sec^{-1}

K_T = the carrier lifetime damage factor, cm^2/sec

and \emptyset = the radiation dose, $\text{electrons}/\text{cm}^2$

Since the recombination rate is the inverse of the carrier lifetime,

(5) may be stated as

$$(6) \quad 1/\tau = 1/\tau_0 + K_t \emptyset$$

where τ = post-irradiation lifetime

and τ_0 = initial lifetime

As the radiation dose, \emptyset , is increased, the initial lifetime, τ_0 , becomes less important.

The following are the advantages of the high-energy radiation technique in controlling the lifetime of silicon diodes: 1) irradiation may be performed on dice alone, 2) there is approximately 80% less reverse leakage at 150°C than for a gold diffused diode with the same t_{rr} and 3) radiation provides a spatially homogeneous distribution of lifetimes throughout the diode. Radiation has proven to be the most controllable process for lifetime reduction.

Two sets of sixteen dice, each from lot NASA-007 were sent out for beta radiation. One set received 12 megarads and the other 16 megarads to provide data points from which to interpolate the correct radiation dose. (Tables 2 and 3) The results indicate that a radiation dose of 14 megarads may be routinely used. This dose produces devices with a high V_F and low t_{rr} . Adjusting the time and temperature of the reflow furnace used during the assembly in the DO-5 package allows the correct V_F to be achieved while retaining a satisfactory t_{rr} .

Device	$V_F @ 50A$	$V_R @ 500uA$	t_{rr}
Number	(Volts)	(Volts)	(Nanoseconds)
168	1.35	1300	250
169	1.33	1270	200
170	1.32	1120	250
171	1.24	1000	250
172	1.27	1260	225

Table 2 Forward voltage drop, blocking voltage
and reverse recovery time of lot NASA-007
devices radiated with 12 megarads β radiation.
(After packaging)

Device	$V_F @ 50A$	$V_R @ 500uA$	t_{rr}
Number	(Volts)	(Volts)	(Nanoseconds)
174	1.42	1260	175
175	1.38	1000	175
176	1.60	750	175
177	1.31	1240	175
178	1.25	1100	200

Table 3 Forward voltage drop, blocking voltage
and reverse recovery time of lot NASA-007
devices radiated with 16 megarads β radiation.
(After packaging)

3.4 Forward Voltage Drop

The voltage drop across the diode in the forward mode consists of five components: N^+-N junction, V_O , P^+-N_i junction, V_I , and the three regions (N^+ , N_i , P^+) V_N , V_i , V_p . See Figure 12.

$$(7) \quad V_F = V_O + V_I + V_N + V_i + V_p$$

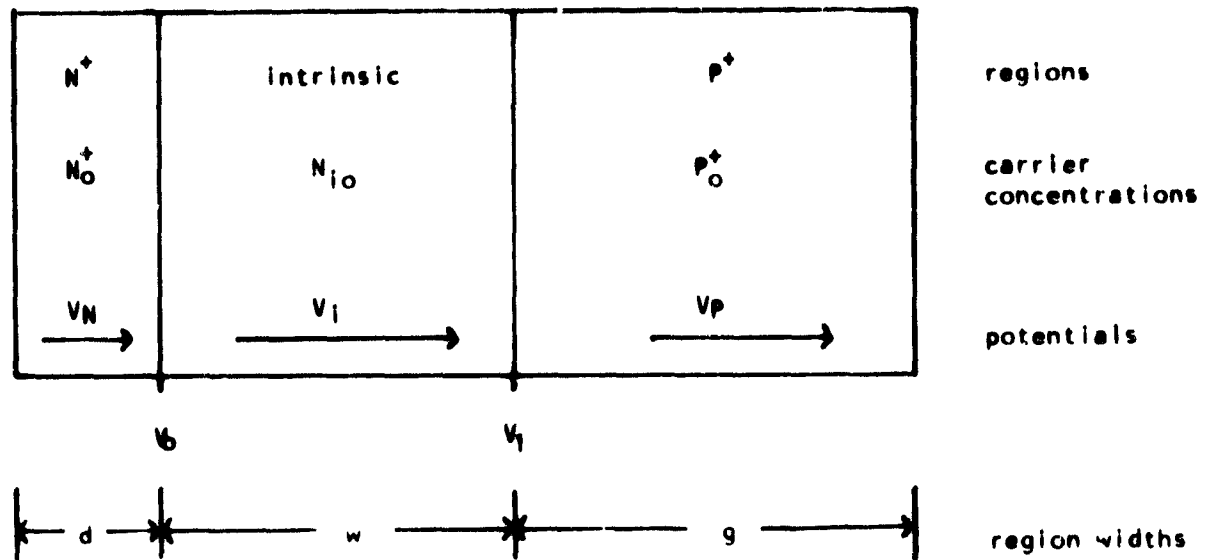


Figure 12 Forward voltage drop

The following analysis is similar to the one found in Reference (4).

The symbols are defined as follows:

d = the width of the N⁺ region = 25 microns

g = the width of the P⁺ region = 137 microns

w = the width of the intrinsic region = 90 microns

q = the electron charge = 1.6×10^{-19} coulombs

D = the diffusion coefficient for holes and electrons

at high carrier concentration, assumed equal =

$6.5/\text{cm}^2\text{sec}$

J = the forward current density = $125 \text{ amps}/\text{cm}^2$ @ 50 amps

N_{i0} = the intrinsic carrier density = 1.5×10^{14} atoms/cc

N_0^+ = the thermal equilibrium carrier concentration

of the N⁺ region = 6.5×10^{19} atoms/cc

P_O^+ = the thermal equilibrium carrier concentration

of the P^+ region = 1.44×10^{19} atoms/cc

$\theta = q/kT = 38.6$ volts $^{-1}$

τ = the carrier lifetime = 2×10^{-7} seconds

μ = the mobility of electrons and holes, assumed equal

= $250/\text{cm}^2\text{sec volt}$

At the $N^+ - N_i$ region, the voltage drop is given by

$$(8) \quad V_O = \frac{1}{2\theta} \ln (J_d N_O^+ / 2 N_{iO}^+ q D)$$

where (9) J_p = the hole current = $q D N_O^+ \psi_O^2 / d = J/2$

and (10) $\psi_O^2 = \frac{N_{iO}^2 e^{2\theta V_O}}{N_O^{+2}}$ is the concentration imbalance

coefficient for this region.

At the $N_i - P^+$ junction, the voltage is given by

$$(11) \quad V_1 = \frac{1}{2\theta} \ln (J_g P_O^+ / 2 q D N_{iO}^2)$$

where (12) J_n = the electron current = $q D P_O^+ \psi_1^2 / g = J/2$

and (13) $\psi_1^2 = \frac{N_{iO}^4 e^{2\theta V_1}}{P_O^{+2} N_O^{+2}}$ is the concentration imbalance

coefficient for the junction.

V_O and V_1 from (1) and (4) may be summed to give the total drop across the 2 regions, V_j :

$$(14) \quad V_j = V_O + V_1 = \frac{1}{\theta} \ln (J (g d P_O^+ N_O^+)^{1/2} / 2 q D N_{iO}^2)$$

In our case the voltage across both junctions, $V_j = 0.542$ volts.

The current through the N^+ region is

$$(15) \quad J = 2 q \mu N(x) E(x)$$

Integrating the electric field, $E(x)$ yields V_N

$$(16) \quad V_N = \int_0^d E(x) dx = \int_0^d \frac{J dx}{2q\mu N_0^+} = 3.2 \times 10^{-5} \text{ volts.}$$

Similarly, the voltage drop through the P^+ region is

$$(17) \quad V_P = \int_0^g \frac{J_g}{2q\mu P_0^+} = 7.01 \times 10^{-3} \text{ volts.}$$

The voltage drop through the intrinsic region is again the integral of the electric field, which is a function of the carrier concentration, which varies through the region.

$$(18) \quad V_I = \frac{J}{2q\mu} \int_0^w \frac{dx}{N(x)}$$

There are 2 functions giving the concentration for each of the two sides of the intrinsic region. See Figure 13.

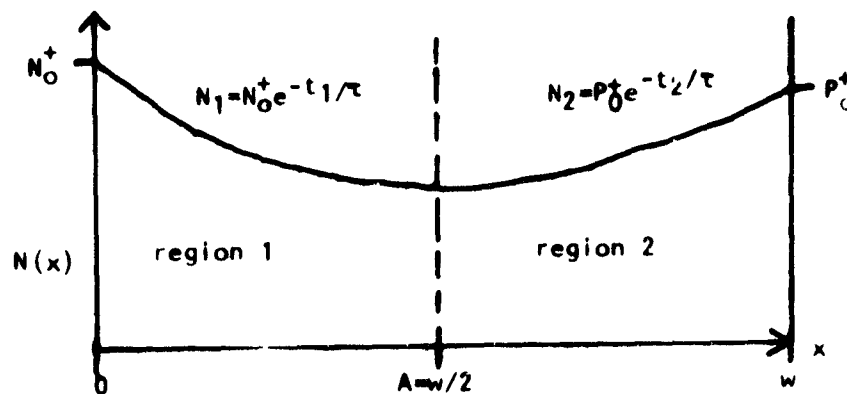


Figure 13 Intrinsic region

At point A, the concentrations given by the two functions are equal and so point A is the transition between the 2 functions.

In region 1,

$$(19) \quad N_1(t) = N_0^+ e^{-t_1/\tau} \text{ is the concentration of carriers on the } N^+ \text{ side of the intrinsic region as a function of the carrier's time in the region, } t_1, \text{ and the carrier lifetime, } \tau.$$

in region 2,

$$(20) \quad N_2(x) = P_0^+ e^{-t_2/\tau} \text{ is the concentration of carriers on the } P^+ \text{ side of the intrinsic region as a function of the carrier's time in the region, } t_2, \text{ and the carrier lifetime, } \tau.$$

which represent exponential decay of carriers from both sides.

The concentrations of holes and electrons are assumed equal in the intrinsic region. The time in the region, t , is given by the distance traveled, x , divided by the average velocity of the carriers, \bar{v} , $t_1 = x_1/\bar{v}$. The average velocity is the current divided by the concentration and carrier charge, $\bar{v} = J/qN_1(x)$. Therefore, in region 1, $t_1 = qx_1N_1(x)/J$ and by the same reasoning in region 2, $t_2 = qx_2N_2(x)/J$. x_1 is the distance from the N^+ boundary and so is just x , x_2 is the distance from the P^+ boundary given by $(w-x)$. We have $t_1 = qxN_1(x)/J$ and $t_2 = q(w-x)N_2(x)/J$.

These give

$$(21) \quad N_1(x) = N_0^+ \exp(-qxN_1(x)/J\tau) \quad \text{for } x < A$$

and $(22) \quad N_2(x) = P_0^+ \exp(-q(w-x)N_2(x)/J\tau) \quad \text{for } x > A$

These may be approximated by

$$(23) \quad N_1(x) = N_0^+ / (1 + qN_0^+x/J\tau)$$

and $(24) \quad N_2(x) = P_0^+ / (1 - qP_0^+(x-w)/J\tau)$

which, when placed in (18) and integrated, yield

$$(25) \quad V_i = \frac{J}{2qu} \int_0^w \frac{dx}{N(x)} = \frac{J}{2qu} \left(\int_0^A \frac{dx}{N_1(x)} + \int_A^w \frac{dx}{N_2(x)} \right) \\ = \frac{J}{2qu} \left(\frac{w}{2P_0^+} + \frac{w}{2N_0^+} + \frac{qw^2}{4J\tau} \left(1 + \frac{N_0^+}{P_0^+} \right) \right)$$

since $A = \frac{w}{2}$ to within a percent

therefore $V_i = 0.836$ volts and

$$V_F = 0.518 + 0.00006 + .00152 + 0.836 = 1.355 \text{ volts}$$

at $I_F = 50$ amps

This voltage is less than that measured across the assembled device at 50 amps which is typically 1.5 volts. The discrepancy may be accounted for by several factors. The ohmic contacts between the chip and the stud, the top contact and chip and the top contact and cap crimp may add 200-300 mv, while the lifetime reducing radiation tends to increase intrinsic resistivity 20-50% due to lattice damage. This increase is in addition to that caused by shortening the carrier lifetime, τ .

3.5 Trade-offs

The major electrical characteristics (forward voltage drop, blocking voltage and reverse recovery time) of this device are inter-dependent. Both the forward voltage drop and the blocking voltage are functions of the intrinsic layer thickness. The peak reverse voltage required determines this thickness and so its contribution to the forward voltage. A lower blocking voltage will give a device a lower forward voltage as seen from Table 1.

A critical trade-off exists between the forward voltage drop and the reverse recovery time. They are inversely coupled; as reverse recovery time decreases, forward voltage increases. The radiation that reduces lifetime disrupts the crystal lattice and so raises the forward voltage. Time spent at temperatures above the annealing temperature of silicon reverses this damage, thereby raising t_{rr} and lowering V_F . This trade-off was advantageous as devices initially too fast and with a V_F too large were reannealed to bring both parameters to acceptable levels.

A third trade-off exists between blocking voltage and t_{rr} since t_{rr} is a function of Q_R , the charge stored in the device after the forward current ceases. The thick intrinsic layer of high voltage devices holds much of this charge and therefore a lower voltage device with a thinner intrinsic layer will be faster than a higher voltage device, all else being the same.

4. WAFER PROCESSING

4.1 Diffusion and Lap & Polish

The $P^+/N^-/N^+$ device profile is formed on 35-40 ohm cm n-type neutron doped silicon material.

Using spin-on liquid boron source, P^+ layers are diffused simultaneously on both sides of the wafer. To achieve the required 5.4 mil junction depth, drive-in diffusion is performed at 1250°C for 264 hours.

The P^+ layer is removed from one side of the wafer by mechanical lapping, followed by chemical polishing to provide adequate surface finish for subsequent moat and cathode geometry formations. The intrinsic material thickness target is 4.5 mils, resulting in 9.9 mils thick wafers after lap and polish.

The N^+ cathode layer is diffused using $POCl_3$ source during one hour deposition at 1130°C, followed by drive-in diffusion targeted for 1 mil N^+ depth on 3.5 mil thick intrinsic N^- region. See Figure 14.

4.2 Positive Bevel Moat

By standard photoresist and masking techniques the moat geometry (Dgw. No. 100003-11, mask No. 2) is defined on the cathode side of the wafer. Silicon dioxide is removed from that area and approximately 5 mil deep moat is etched to form the positive

bevel junction. Figures 6 and 14.

4.3 Glass Passivation

High temperature glass, suspended in a binder, is deposited in the freshly etched and cleaned moat. In a two step furnace processing the binder is burned off and the glass is fired at 730°C and fused to the walls of the moat. To assure complete and continuous glass passivation of the high voltage junction, the glass deposition and firing process is performed twice.

4.4 Metallization

A metallization process that is compatible with glass passivated junctions and provides solderable contacts to cathode and anode has been developed. These contacts have series voltage drops comparable to the standard aluminum and gold contact systems.

The new metallization is a tri-metal system, consisting of aluminum, titanium and nickel. The metals are evaporated in a high vacuum equipment. Aluminum is deposited first. A thin layer of titanium is flashed on the aluminum to act as a binder between the aluminum and nickel. A layer of nickel provides the solderable contact. The cathode contact areas are defined by standard photoresist and masking (Dwg. No. 100003-11, mask No. 3) techniques and selective etching. On the anode side of the wafer a continuous metallization of the same system is deposited.

The contacts are sintered in a nonoxidizing ambient to establish low resistance ohmic contacts between the aluminum and silicon surfaces.

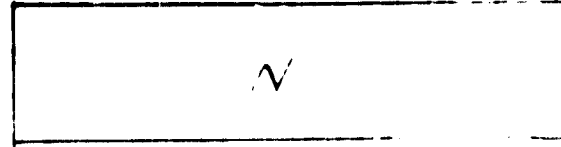
4.5 Wafer Test and Dicing

To complete the wafer processing, 100% wafer probing is performed to test for minimum acceptable blocking voltage.

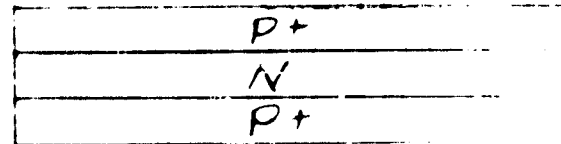
The wafers are diamond saw cut into the hexagonal geometry dice, sorted for electrical and mechanical acceptance and delivered for assembly.

PROCESS SEQUENCE OUTLINE

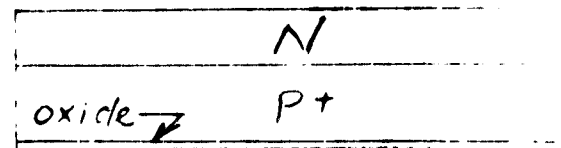
1. STARTING MATERIAL WAFER NEUTRON DOPED N-TYPE SILICON



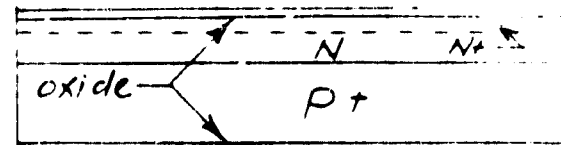
2. BORON DEPOSITION AND DRIVE IN DIFFUSION



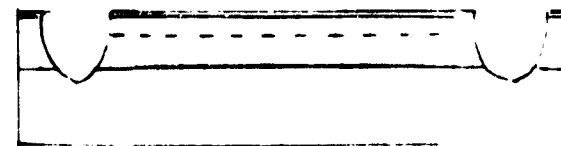
3. SINGLE SIDE LAP & POLISH OXIDATION (ONE SIDE)



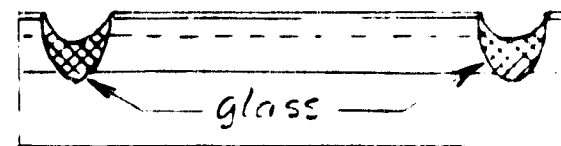
4. PHOSPHORUS DEPOSITION AND DRIVE-IN DIFFUSION



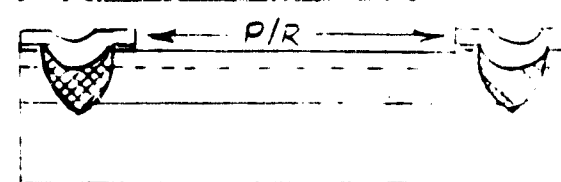
5. PHOTORESIST MASK, OXIDE AND MOAT FORMATION ETCH



6. HARD GLASS PASSIVATION IN THE MOAT



7. CONTACT PHOTORESIST AND OXIDE ETCH



8. ANODE AND CATHODE FOUR LAYER METALLIZATION

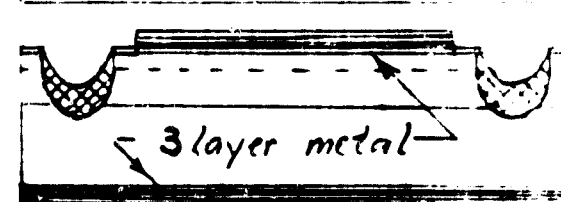


FIGURE 14

5. ENCAPSULATION

5.1 Package

The device is encapsulated in JEDEC standard DO-5 assembly, utilizing soft solder reflow process and hermetically sealed by resistance welded cap. The diode is assembled in the reverse polarity, i.e., DO-5 stud is the anode and the cap terminal is the cathode.

The specifications of the assembly components are detailed in the following drawings:

DO-5 stud - Impex, 1404

DO-5 cap - 50-0016

Moly tab, cathode - 50-0003-4

Moly tab, anode - 50-0003-3

Internal lead - 50-0011

Solder preform, cathode - 50-0004-7

Solder preform, anode - 50-0004-6

5.2 Assembly

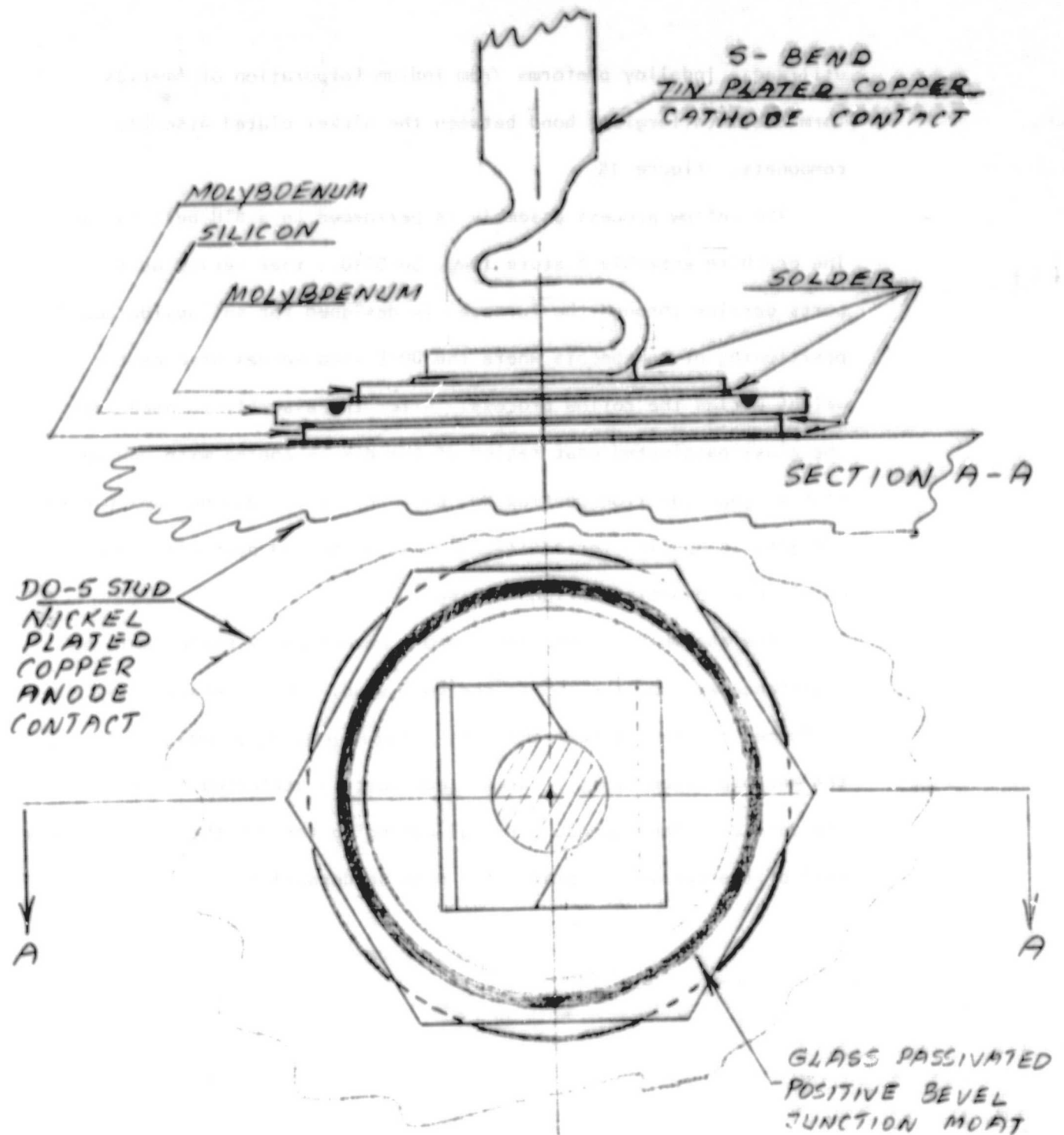
In one-pass solder reflow process the die is mounted on the nickel plated stud platform and the internal lead attached. For improved coefficient of expansion matching between the silicon material and copper electrodes, molybdenum back-up plates are

utilized. Indalloy preforms from Indium Corporation of America form the metallurgical bond between the nickel plated assembly components. Figure 15.

The reflow process assembly is performed in a BTU belt furnace. The graphite assembly fixture (Dwg. 50-0010), that serves as the parts carrier through the furnace, is designed for an "Upside-down" positioning of components where the D0-5 stud serves also as the weight during the reflow process. After the assembly furnace pass, the glass passivated moat region of the die is coated with Dow Corning high voltage junction coating No. 643. Prior to capping, Dow Corning RTV 3140 is applied for additional insulation and protection against possible weld arcing during capping.

The assembly is completed into a hermetically sealed unit by resistance welding the cap to the D0-5 stud. This operation is performed in dry nitrogen ambient, achieving inert conditions inside the encapsulation cavity. Gross leak test is performed for 100% of the devices. The cathode terminal extending through the glass to metal seal of the cap is tin plated for good solderability.

SOLDER REFLOW ASSEMBLY
REVERSE POLARITY
DIODE



APPROXIMATE SCALE 10:1

FIG. 15

ORIGINAL PAGE IS
OF POOR QUALITY

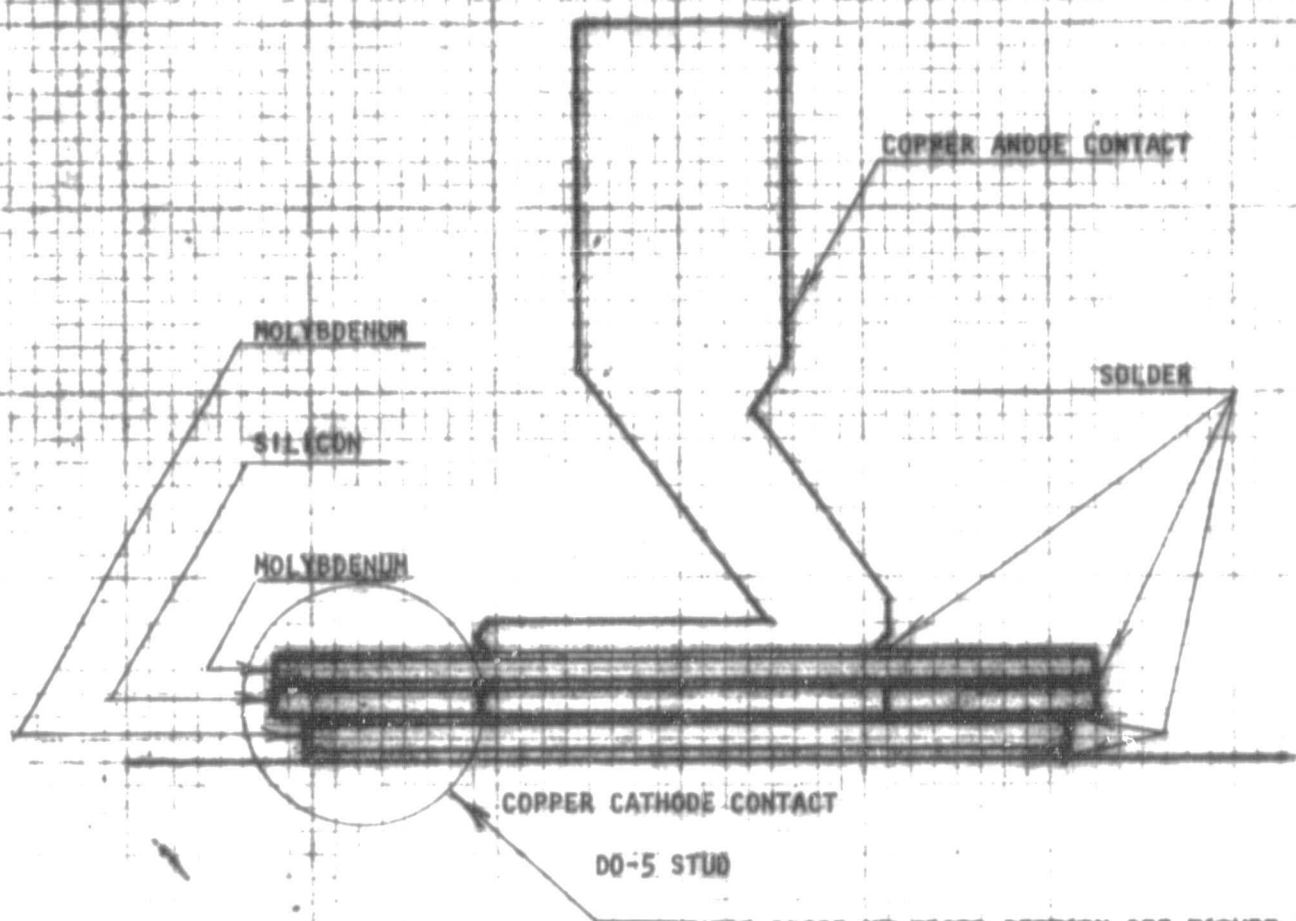
5.3 Polarity Trade-off

The initial proposal specified a normal polarity assembly, i.e., cathode mounted on the D0-5 stud and the cap terminal serving as the anode contact. (Figures 16 & 17) A large number of the assembled 1000-1400 volt units exhibited corona effect between the positive bevel moat region and the moly cathode back-up plate. The use of Dow Corning high voltage semiconductor junction coating No. 643 had only limited success because of the narrow access spacing between the surfaces to be isolated.

This problem could not be reliably eliminated without a major change in the D0-5 stud design; therefore, it was agreed that the contract be completed on time with the diode assembled in the reverse polarity, as shown in Figure 15 and described in the assembly process.

The D0-5 stud base that is proposed for the normal polarity assembly to be investigated, is available from the Nipert Company as P/N 068-8903-05. The pedestal of the cold formed copper stud with the brazed molybdenum back-up plate provides 0.060 inch clearance between the main body of the stud and the surface area of the silicon die extending over the pedestal. This clearance provides sufficient space for applying high voltage dielectric coating to the exposed surfaces of the silicon die and the cathode stud, thereby eliminating arcing. Figure 18.

SOLDER REFLOW ASSEMBLY

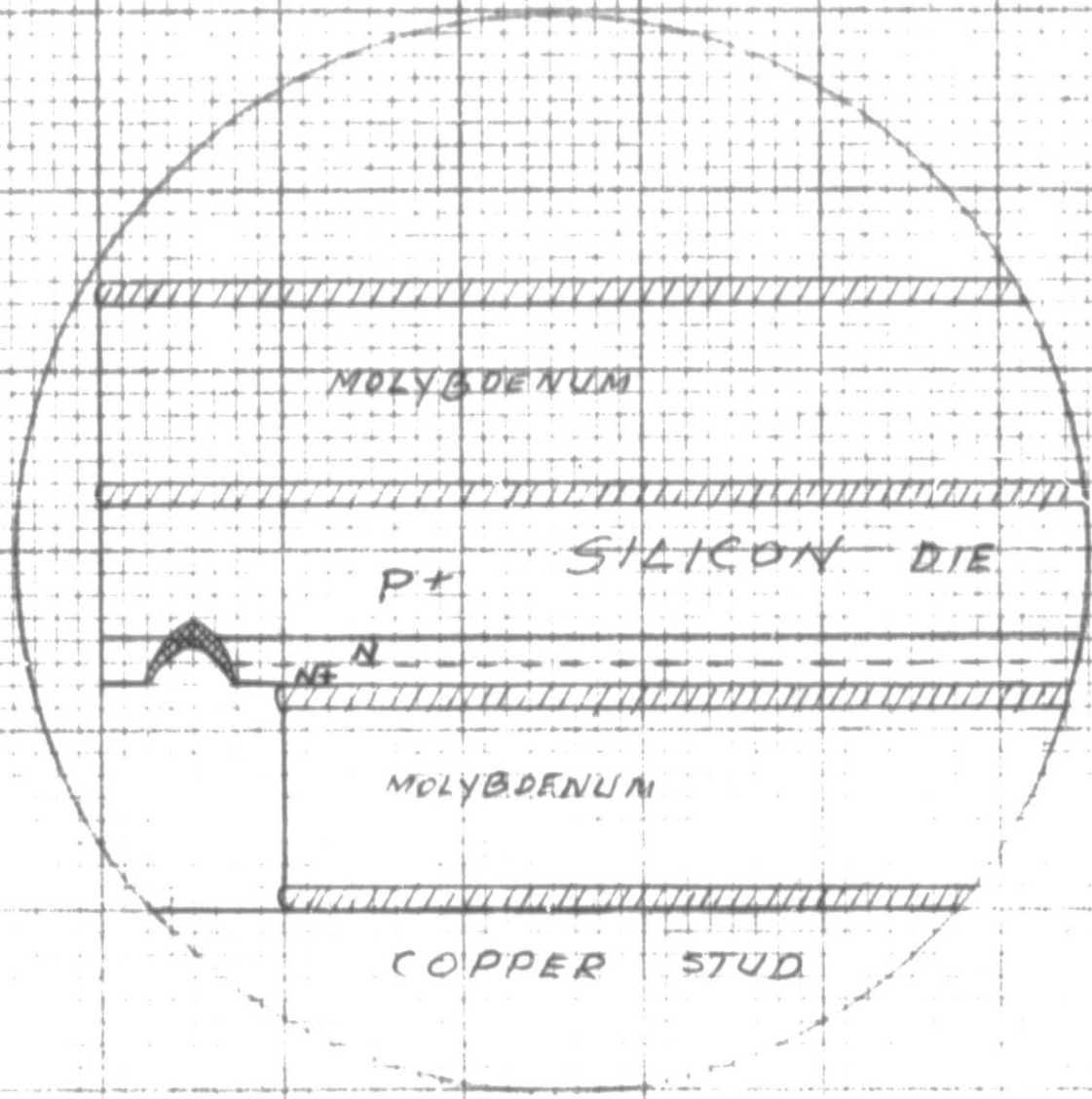


FOR CLOSE-UP CROSS SECTION SEE FIGURE 5.

FIGURE 16

ORIGINAL PAGE IS
OF POOR QUALITY

CLOSE-UP CROSS SECTION FROM FIGURE 16



 — HARD GLASS
 — SOLDER

FIGURE 37

NORMAL POLARITY ASSEMBLY
(MODIFIED VERSION)

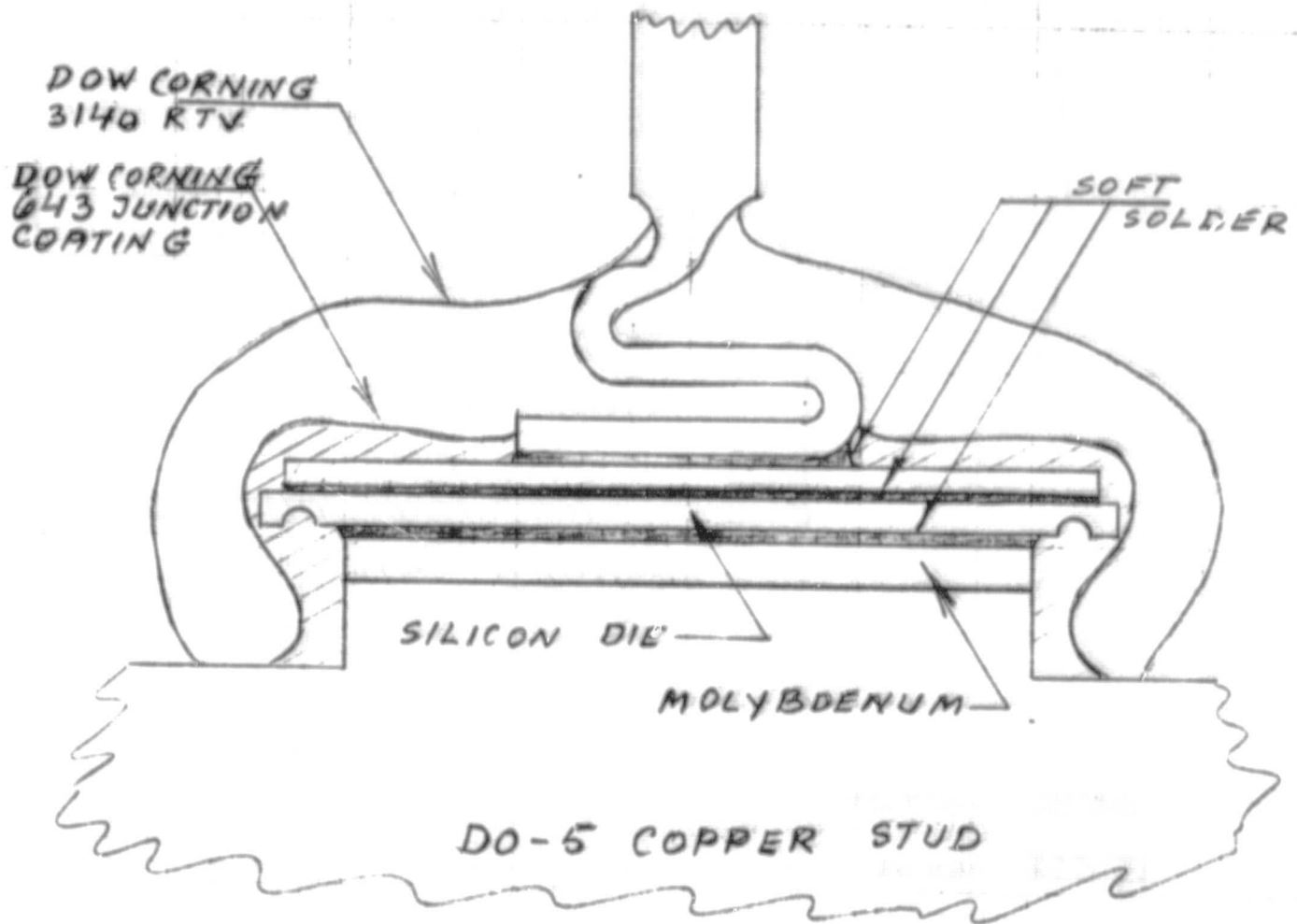


FIGURE 1B.

5.4 High Voltage Cap

New D0-5 cap designed to comply with Underwiter's Laboratories specifications for high voltage devices has been designed (Dwg. No. 50-0017) and fabrication funded by Power Transistor Company. The standard D0-5 glass-to-metal seal is replaced by ceramic-to-metal assembly. This design provides insulation between the anode and the cathode of 0.625 inch minimum surface length in any direction.

5.5 Thermal Ratings

Junction temperature is determined by the total power dissipation in the device P_T , the ambient or case temperature T_C , and the thermal resistance θ_{JC} from junction to case.

$$(26) \quad T_J = T_C + \theta_{JC} P_T$$

The basic equation for the conduction of thermal energy is

$$(27) \quad Q = \frac{KA}{L} \Delta T = \frac{KA}{L} (T_1 - T_2)$$

where Q = heat flow/unit of time

K = thermal conductivity constant, W/cm, $^{\circ}\text{C}$

A = area of thermal path, cm^2

L = length of thermal path, cm

T_1 = temperature of heat source, $^{\circ}\text{C}$

T_2 = temperature of heat sink, $^{\circ}\text{C}$

rewritten (27)

$$(28) \quad Q = \frac{T_1 - T_2}{L/KA} = \frac{T_1 - T_2}{\theta}$$

and

$$(29) \quad \theta = \frac{L}{KA}$$

The thermal spreading is taken into consideration by applying the following equation for circular geometry:

$$(30) \quad \theta_{\text{circle}} = \frac{L}{K \cdot (r^2 + rL)}$$

where r = radius of the circle

The equivalent diagram in Figure 19 shows the thermal conductive path considered and the calculated theoretical values of each thermal resistance element.

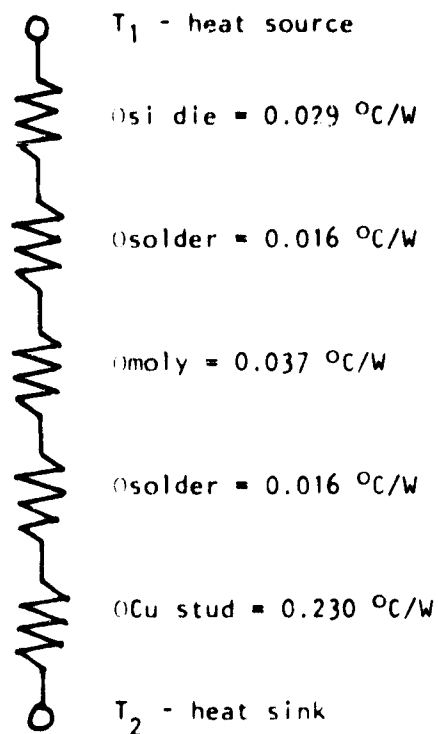


Figure 19 Thermal resistance, equivalent diagram

The resulting junction to case thermal resistance, θ_{JC} is $0.33^{\circ}\text{C}/\text{W}$

6. TEST

6.1 Test Plan

1. Expose all diodes to 1000A non-repetitive peak surge current
2. Screen on Mastech 216 automatic tester for
 - a) $I_R = 100 \mu A$ MAX. @ 1000v
 - b) $V_F = 1.51v$ MAX. @ 50A
3. Serialize and trademark
4. Read and record reverse recovery time at $T_C = 100^\circ C$
5. Read and record forward voltage at $I_F = 50A$
6. Read and record DC blocking voltage at $T_C = 25^\circ C$ and $T_C = 150^\circ C$
7. Read and record maximum reverse current at rated V_{RRM} and $T_C = 25^\circ C$ and $T_C = 150^\circ C$
8. Select deliverable diodes that meet the "specifications"
9. Select samples and generate characteristic curves for
 - a) capacitance versus reverse voltage
 - b) forward voltage versus forward current
 - c) reverse current versus reverse voltage as a function of temperature

The required specification read and record data of the deliverable diodes is tabulated in Table 4. The test equipment and procedures of the tests are discussed in the following paragraphs.

6.2 Non-Repetitive Peak Surge Current, I_{FSM}

As a potentially destructive test I_{FSM} has been performed to screen all devices prior to serializing and performing any other tests. All devices were exposed to 1100A half-cycle surge to insure compliance with the 1000A requirement.

The major components of the peak surge test equipment are: high current variac, SCR and SCR pulse firing circuit, transformer with a high current secondary, current sensing resistor, and oscilloscope, connected as shown in Figure 20.

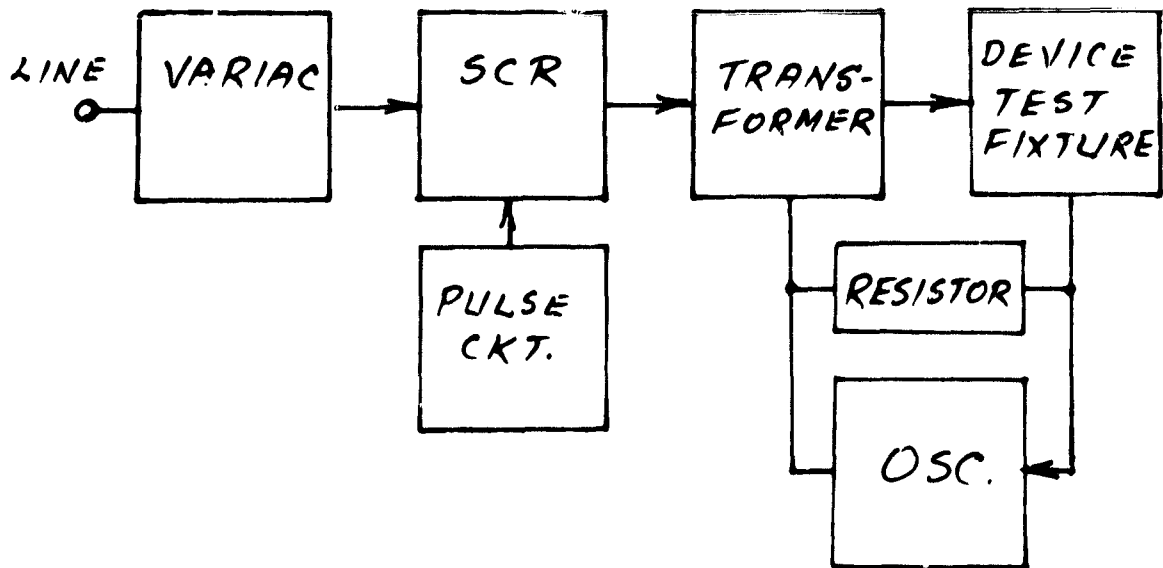


Figure 20
Test Circuit Block Diagram

The device under test is clamp-held in a safety test fixture, Figure 21, while a high current pulse, triggered by the SCR firing circuit, is applied. The amplitude of the current pulse is determined by observing the voltage pulse across the non-inductive one milliohm resistor in series with the diode, as displayed on the oscilloscope. Figure 22. The variac is adjusted for the required pulse amplitude.

Following the high current surge test, a survivor screening test was performed using Mastech 216 automatic tester. At room temperature the diodes were tested for

$$I_R = 100 \mu A \text{ MAX @ } 1000 \text{ volts}$$
$$\text{and } V_F = 1.51 \text{ v MAX @ } 50 A$$

Units that passed the series of tests were serialized for the subsequent read and record tests.

6.3 Reverse Recovery Time, t_{rr}

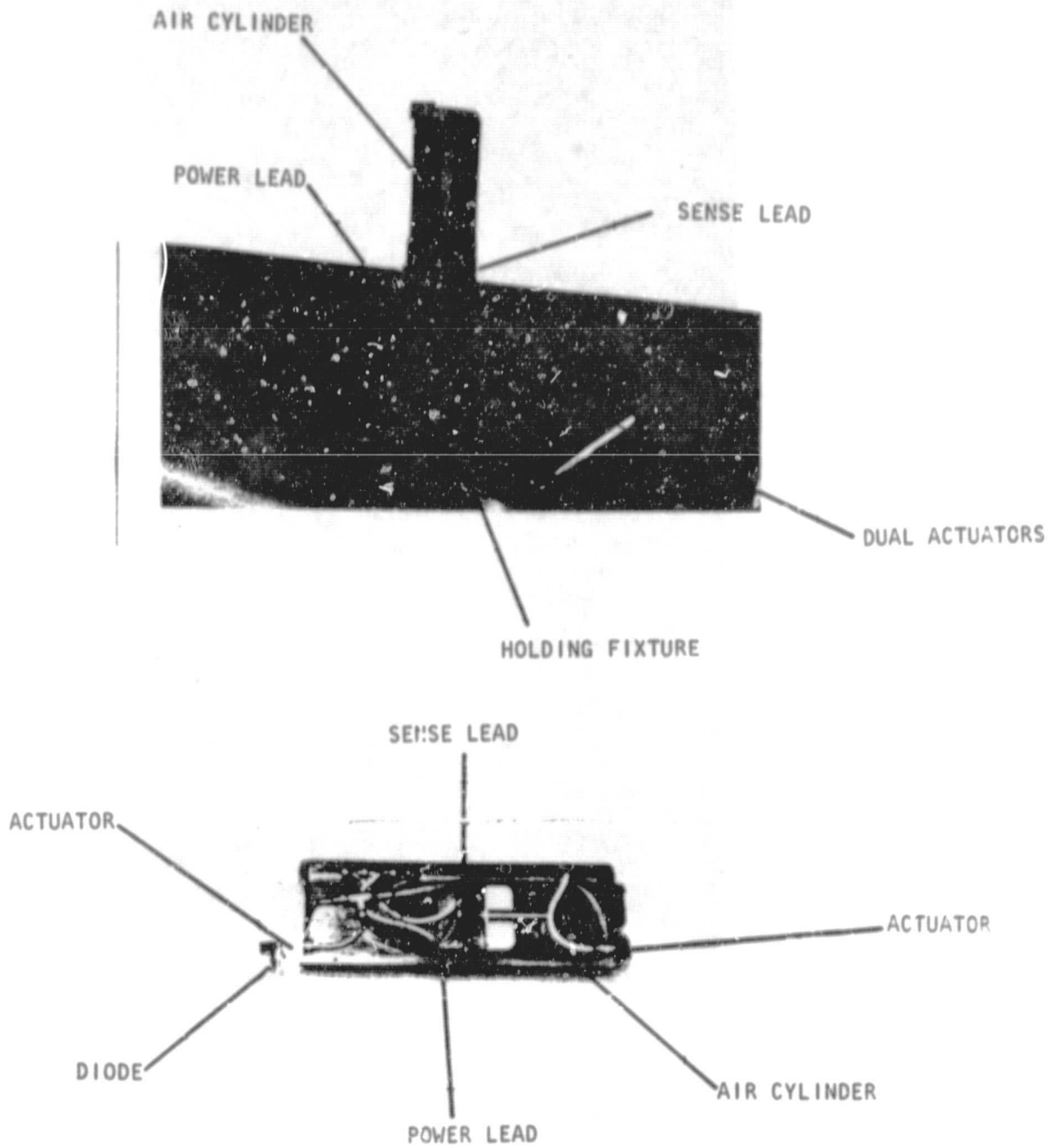
The reverse recovery test was performed in a JEDEC type test circuit.

The current through the diode is reduced at a rate of 25A/sec. When the sign of the current through the diode changes, zero reference line is established. The measurement of the reverse recovery time is made from that point (t_0) to its maximum negative value (t_1) and to the approximate point where the reverse current has returned to 10% of its maximum value, $I_{RM}(REC.)$. See Figure 23.

The diodes were stabilized at 100°C in an oven. Using the reverse recovery test circuit, set at $I_{FM} = 50 A$ and $di/dt = 25 A/\mu sec$.

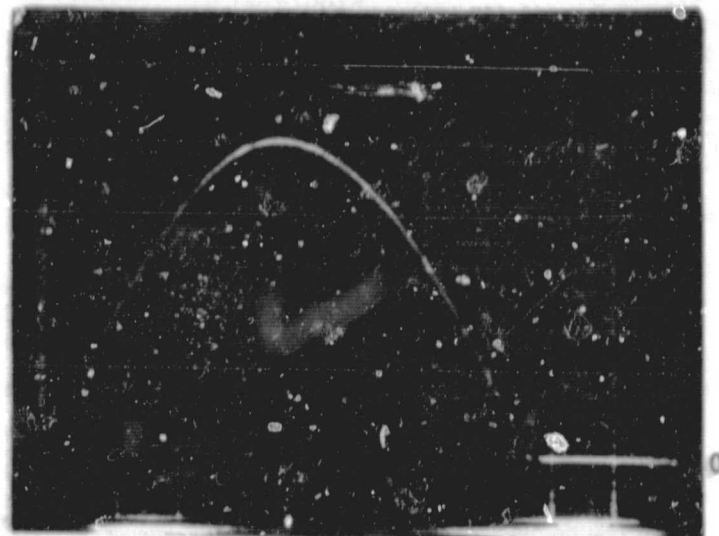
DIODE TESTING FIXTURE

Figure 21



200A/Vert Div

3/19/81

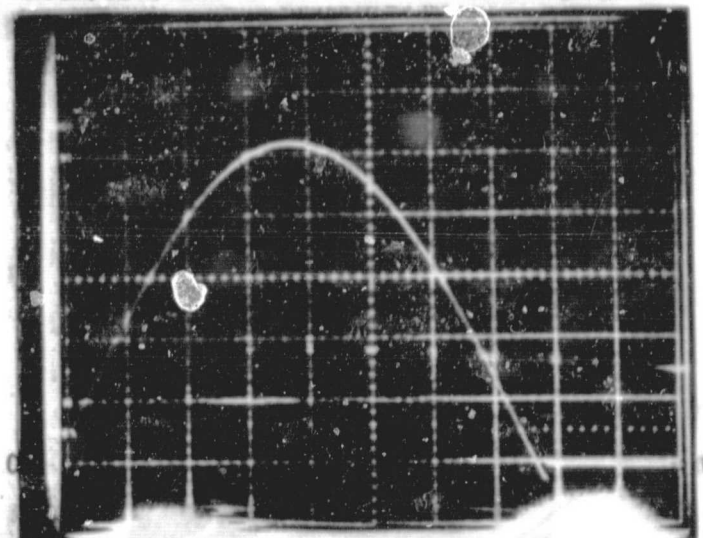


1ms/Horz Div

NASA #112

200A/Vert Div

3/19/81



1ms/Horz Div

NASA #113

Figure 22 Peak surge current pulse

the t_{rr} was read on Tektronix 465 oscilloscope and recorded for each unit.

The t_{rr} test utilizes Tektronix CT5 high current transformer with P6021 current probe. During the performance and the evaluation of the test it was determined that the response limitations of the probe resulted in some loss of accuracy in the oscilloscope reading. Due to some saturation at 50A and even lower current levels the zero reference line is shifted slightly from the initial setting, causing an error in the reading. The upper limit of the probe frequency response rating (20MHz), reduces the accuracy of the time measurement during the very fast recovery from t_1 to t_2 , Figure 23. At 20 MHz the period is 50ns, and the accuracy of reading the time during that segment of recovery is limited to about 100ns. Figure 24.

To eliminate the inaccuracy of this test, new test equipment is being designed to read the current in terms of a voltage directly across a non-inductive resistor in series with the diode under test.

To indicate the true performance of the device, two data points have been logged:

- t_1 - the time from the sign change of the recovery current at t_0 to its maximum negative value,
- t_2 - the time from t_0 to the approximate point where the reverse recovery current has returned to 10% of its maximum value. See Figures 23 and 24.

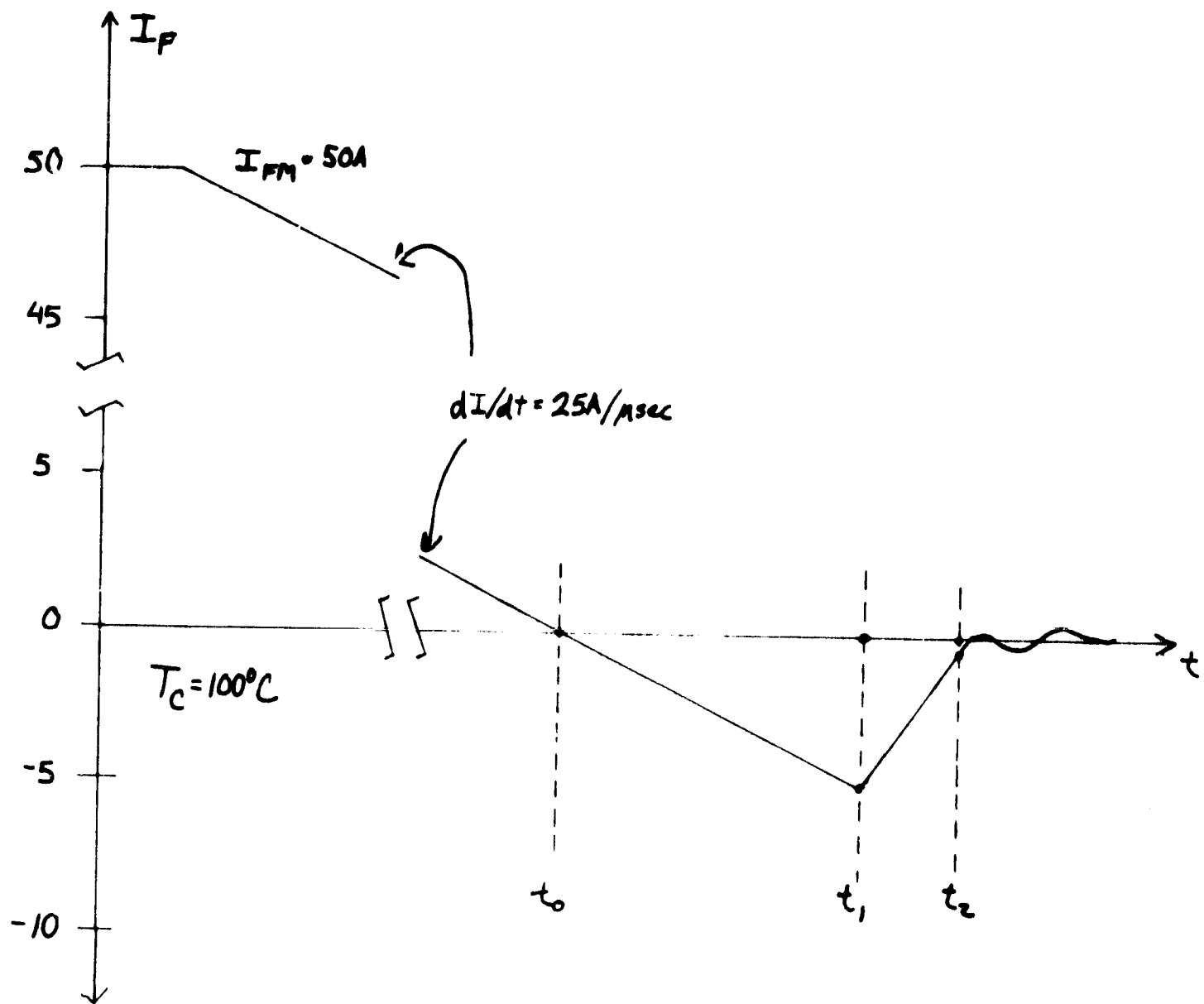
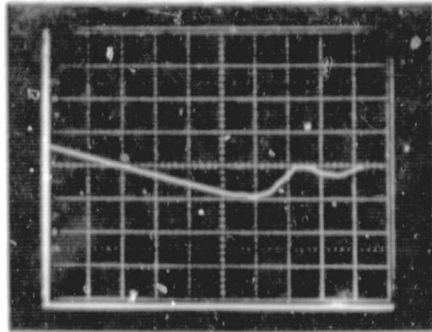
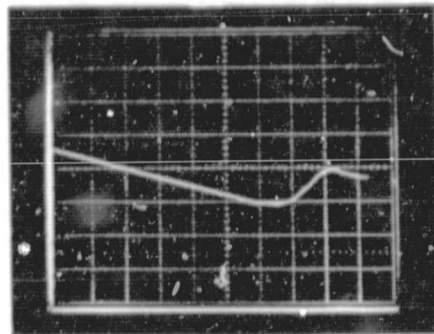


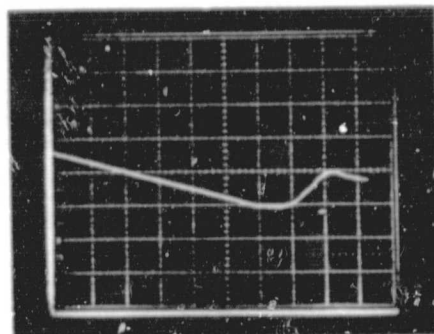
Figure 23 - Reverse recovery waveform



Device #031



Device #038



Device #060

ORIGINAL PAGE IS
OF POOR QUALITY

Vertical Scale: 4A/div

Horizontal Scale: 50 nsec/div

Figure 24 Typical T_{rr} waveforms

Device No.	V _F @ 50A Volts	V _R @ 500 μ A T _C = 25°C Volts	V _R @ 5mA T _C @ 150°C Volts	I _R @ 1000V T _C = 25°C μ A	I _R @ 150°C 800V 1000V μ A	T _{rr} from 50A di/dt = 25A/ μ sec @ 100°C, t ₁ /t ₂ nsec
002	1.49	1225	1350	2	350	325/500
010	1.40	1330	1280	3	300	400/500
012	1.39	1350	1260	2	250	400/500
013	1.32	1200	1280	2	150	400/500
014	1.50	1290	1300	3.5	450	300/425
019	1.46	1340	1380	1.5	1000	325/450
020	1.44	1345	1180	6	1350	350/450
024	1.30	1370	1280	1.5	750	500/600
026	1.44	1160	1285	2	700	325/425
027	1.41	1390	1180	5	1200	400/500
029	1.48	1350	1300	2.5	750	300/400
033	1.46	1340	1260	2	1000	300/400
036	1.48	1360	1410	4	900	350/450
038	1.50	1330	1400	10	1000	275/350
039	1.50	1225	1280	9	1100	275/350
040	1.53	1320	1200	8	1300	275/350
044	1.49	1160	1180	12	1000	350/450
045	1.42	1315	1350	5	500	350/450
047	1.37	1195	1160	1.5	500	275/350
048	1.41	1300	1200	2	600	250/325
049	1.46	1215	1240	12	1100	275/350
050	1.52	1190	1300	3	1000	275/350
051	1.31	1160	1240	10	750	350/400
052	1.48	1360	1350	2.5	900	275/350
053	1.52	1340	1300	10	850	250/350
054	1.51	1325	1340	7	700	250/325
056	1.44	1140	1265	2	700	250/300
058	1.42	1130	1200	8	1800	250/300
059	1.38	1200	1260	6.5	2200	275/350
060	1.42	1250	1280	6	1100	275/350
061	1.45	1320	1350	2	700	280/340
062	1.54	1290	1260	5.5	2000	325/400
066	1.37	1275	1330	4	700	280/340
067	1.45	1280	1380	3.5	1400	325/400
068	1.42	1320	1340	2	850	280/330

Table 4

Device No.	V_F @ 50A Volts	V_R @ 500 μ A $T_C = 25^\circ\text{C}$ Volts	V_R @ 5mA T_C @ 150°C Volts	I_R @ 1000V $T_C = 25^\circ\text{C}$ μA	I_R @ 150°C μA	T_{rr} from 50A $di/dt = 25\text{A}/\mu\text{sec}$ @ 100°C , t_1/t_2 nsec
069	1.39	1310	1200	6	2200	300/400
070	1.50	1295	1320	7	1500	300/400
071	1.48	1290	1350	1.5	550	250/300
072	1.49	1340	1300	4	1400	275/325
074	1.43	1315	1275	11	1500	260/325
075	1.49	1210	1360	5	1000	275/325
077	1.45	1340	1300	3	800	275/325
078	1.48	1295	1320	8	1600	275/325
079	1.53	1250	1370	5	900	275/350
080	1.43	1330	1280	4	850	250/310
081	1.48	1370	1400	4	600	300/450
083	1.50	1340	1400	7	900	300/400
086	1.49	1440	1310	45	1600	275/350
087	1.46	1440	1420	12	1350	325/450
088	1.47	1200	1330	1.5	300	300/400
089	1.43	1330	1320	10	1450	300/400
092	1.46	1230	1340	2.5	500	275/400
094	1.50	1330	1300	6.5	1400	250/350
096	1.36	1265	1360	20	500	350/500

Table 4 (cont'd)

6.4 Forward Voltage, V_{FM}

The Mastech 216, using the digital readout option, was employed to read and record the forward voltage drop at $I_F = 50A$. A typical V_{FM} characteristic trace is shown in Figure 25, as displayed on the Tektronix 576 curve tracer.

6.5 DC Blocking Voltage, V_R

The blocking voltage at $25^{\circ}C$, $500 \mu A$ and at $150^{\circ}C$, $5 mA$ was read on Tektronix 576 curve tracer.

6.6 Reverse Current, I_R

Utilizing Tektronix 576 curve tracer in the Leakage Mode, the reverse leakage current was recorded for $V_R = 100$ volts at $T_C = 25^{\circ}C$ and for $V_R = 800$ volts and 1000 volts at $T_C = 150^{\circ}C$.

All high temperature characteristics were read and recorded with the devices heated in an oven and stabilized at the required elevated temperature.

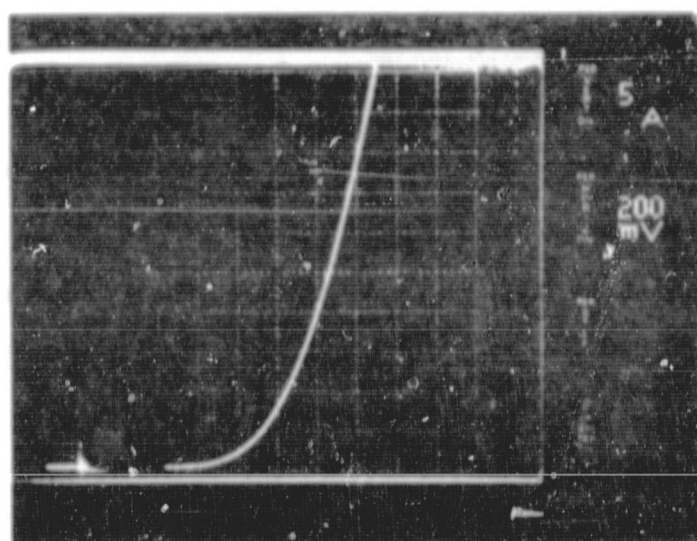


Figure 25
Forward Voltage, V_F

7. ELECTRICAL PERFORMANCE

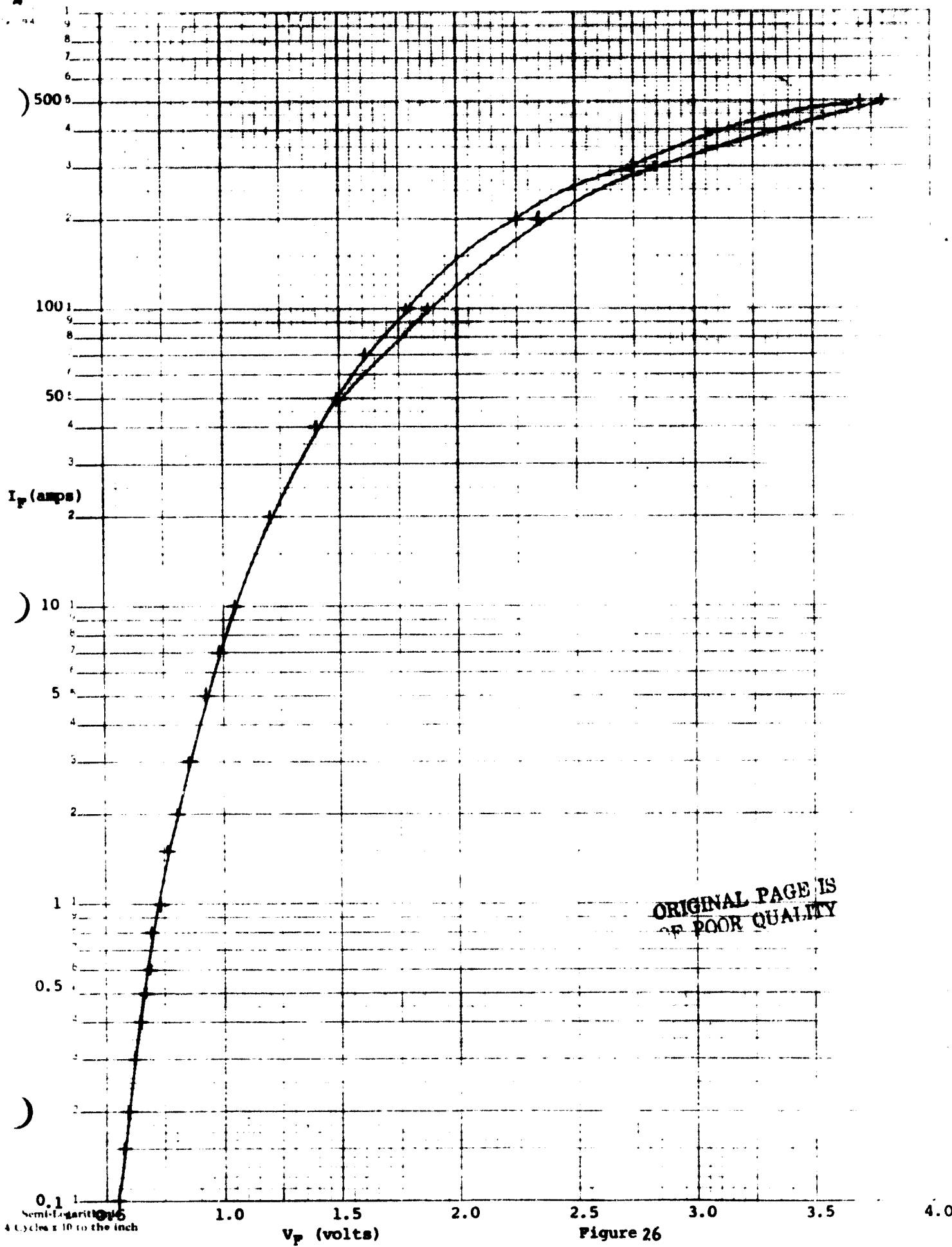
7.1 Characteristic Curves

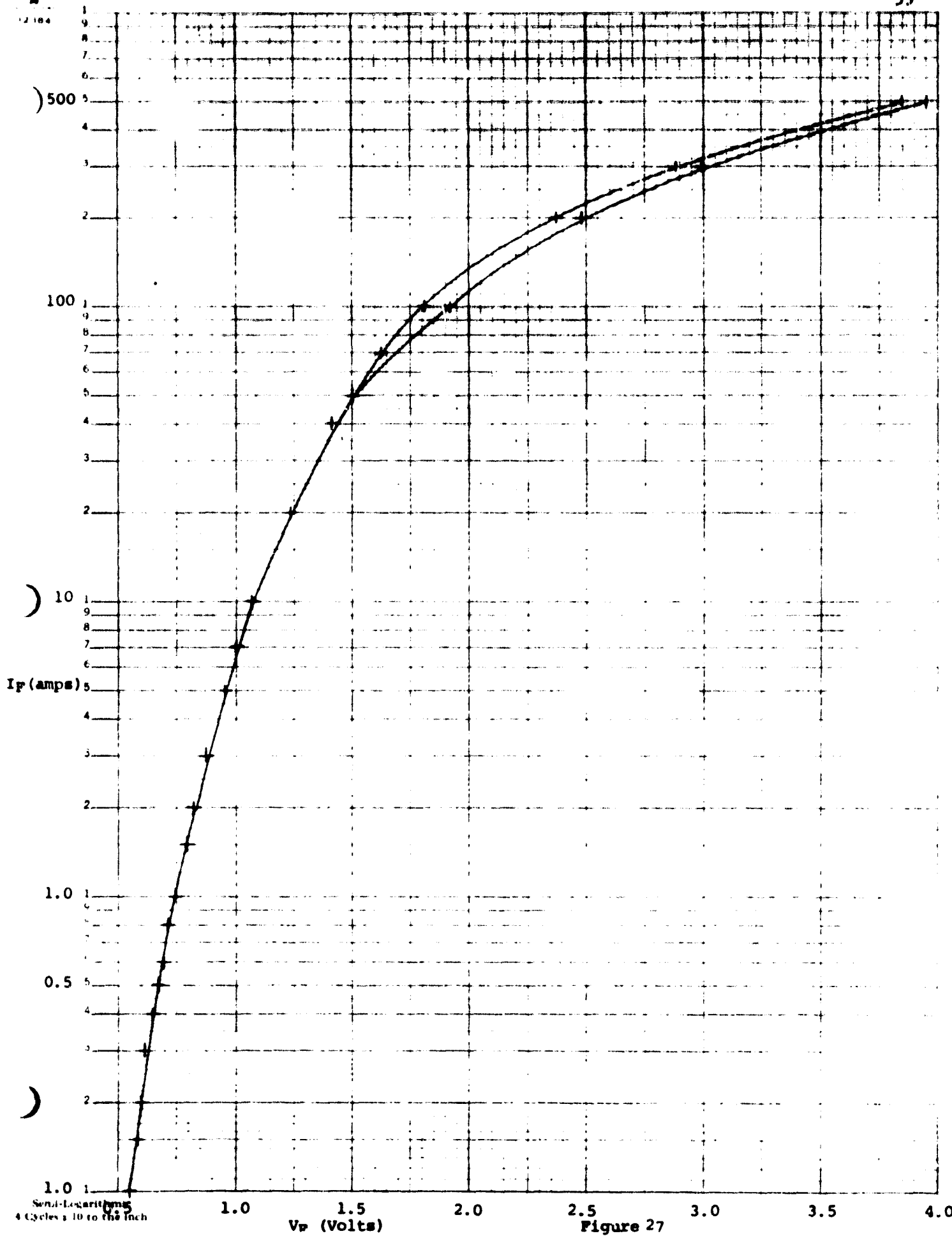
Five devices, numbers 031, 038, 039, 046 and 060 were chosen as typical of the lot and three characteristic curves were generated for each device; forward voltage drop versus forward current (Figures 26-30), reverse leakage current versus reverse voltage at six temperatures (Figures 31-35), average leakage current versus temperature of the five units (Figure 36), and capacitance versus reverse voltage (Figures 37-41).

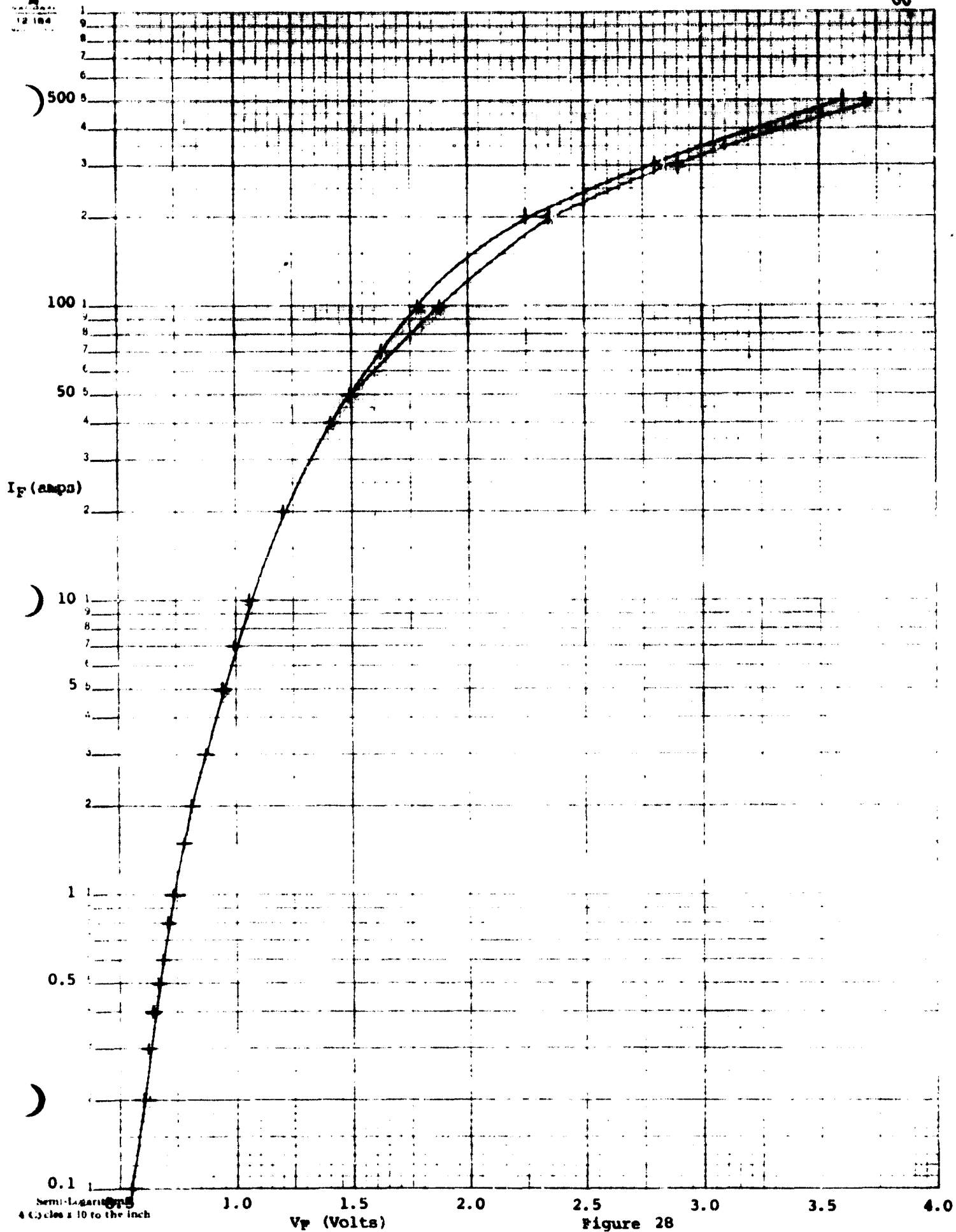
V_F versus I_F was plotted from 100 mA to 100A using the Mastech. V_F for I_F of 100, 200, 300 and 500 amps was found by adjusting the surge current tester to deliver a peak current of the correct value and then displaying the voltage across the device on an oscilloscope. The voltage at 100A was higher when measured with the surge tester than when measured by the Mastech. This implies that the higher current level voltages are offset. The affect was determined to be caused by ohmic drops through the sense wires of the surge test fixture. Therefore, the high current data points have been normalized based on the offset at 100A. Curves have been drawn through both the normalized and the measured points. The actual curves lies between these curves.

The leakage current versus reverse voltage curves were generated by heating the diodes in an oven, stabilizing and then measuring the leakage at 200, 400, 600, 800 and 1000 volts on a 576 curve tracer. The curves that result are straight lines on a semi-log graph whose slopes are independent of temperature. By plotting the average leakage current of the devices at 800 volts against temperature on a semi-log graph, a straight line results which indicates the leakage increases exponentially with temperature (Figure 11).

Capacitance was plotted against reverse voltage by using a Boonton model 72BD capacitance meter and a Hyland high voltage power supply. The resulting curve is a straight line on logarithmic graph paper. The capacitance plot was terminated at 600 volts due to the maximum limitations of the test equipment.







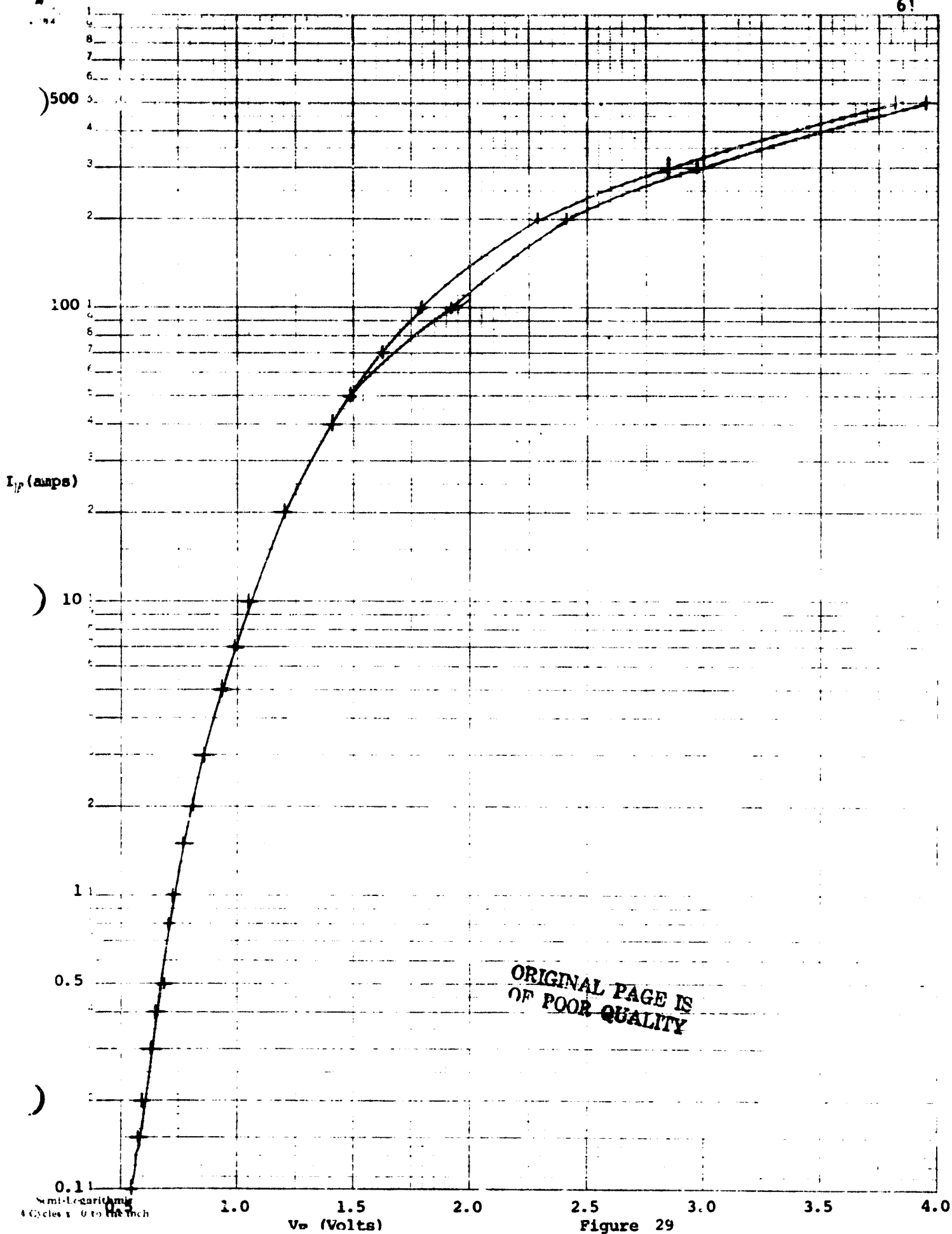
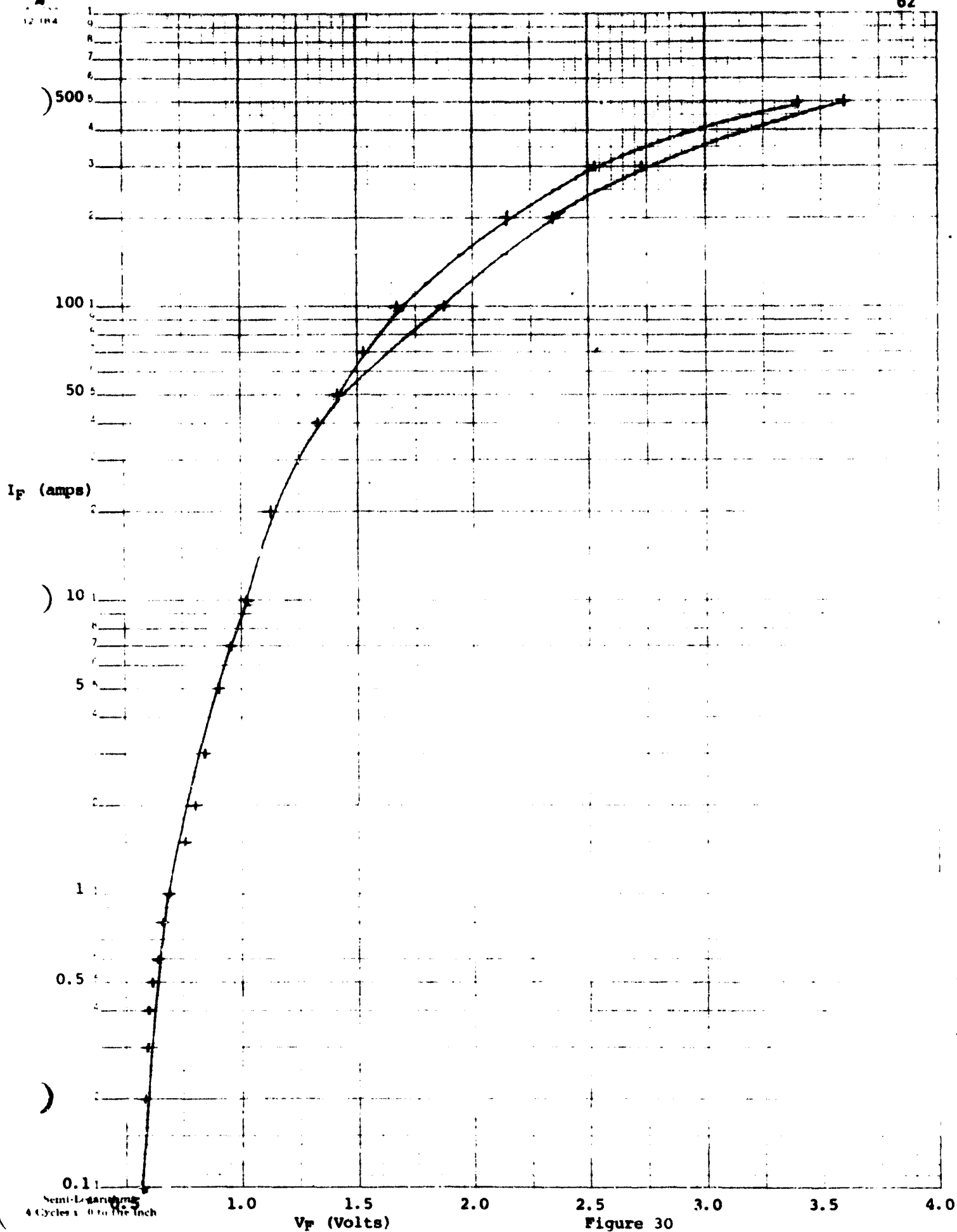


Figure 29



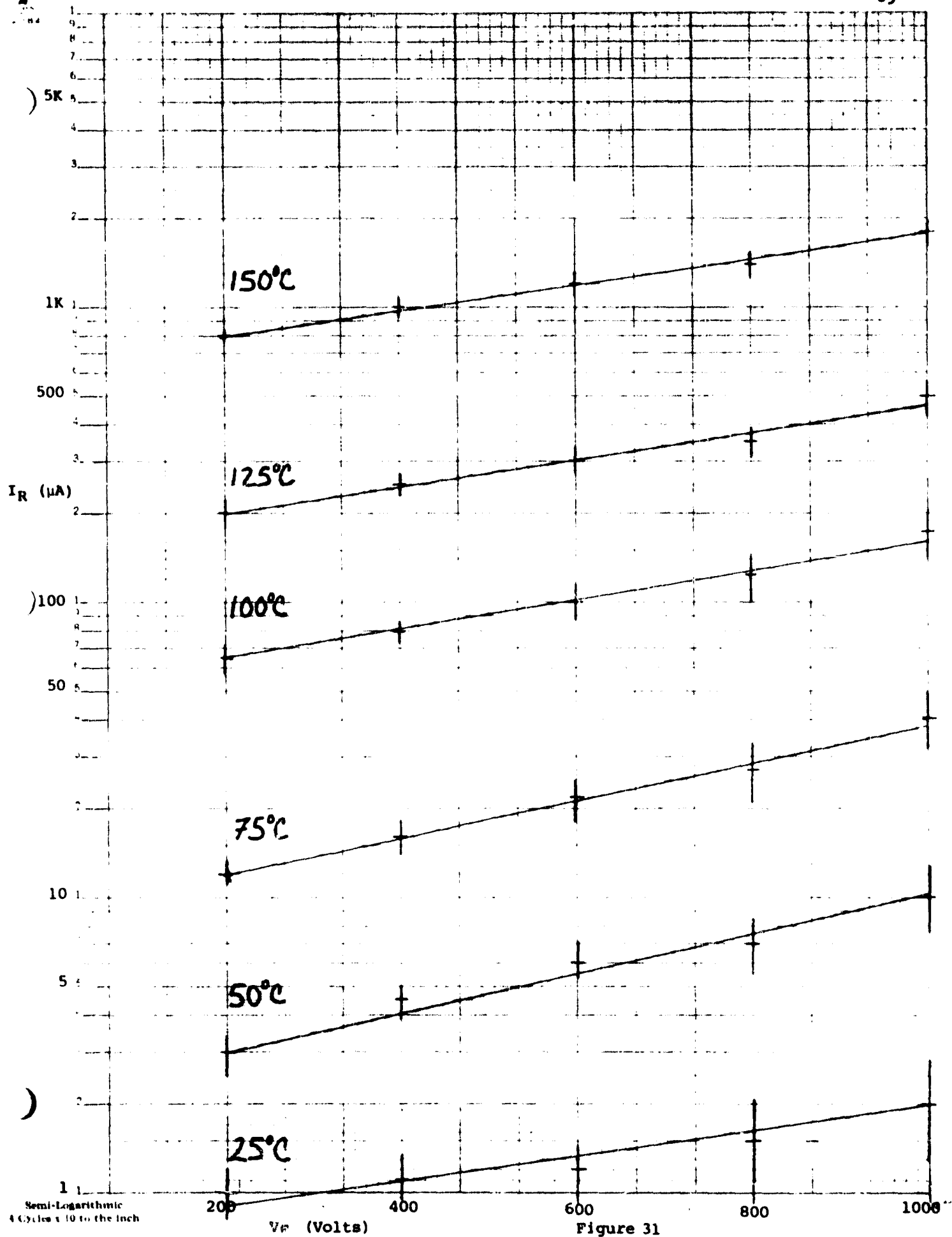


Figure 31

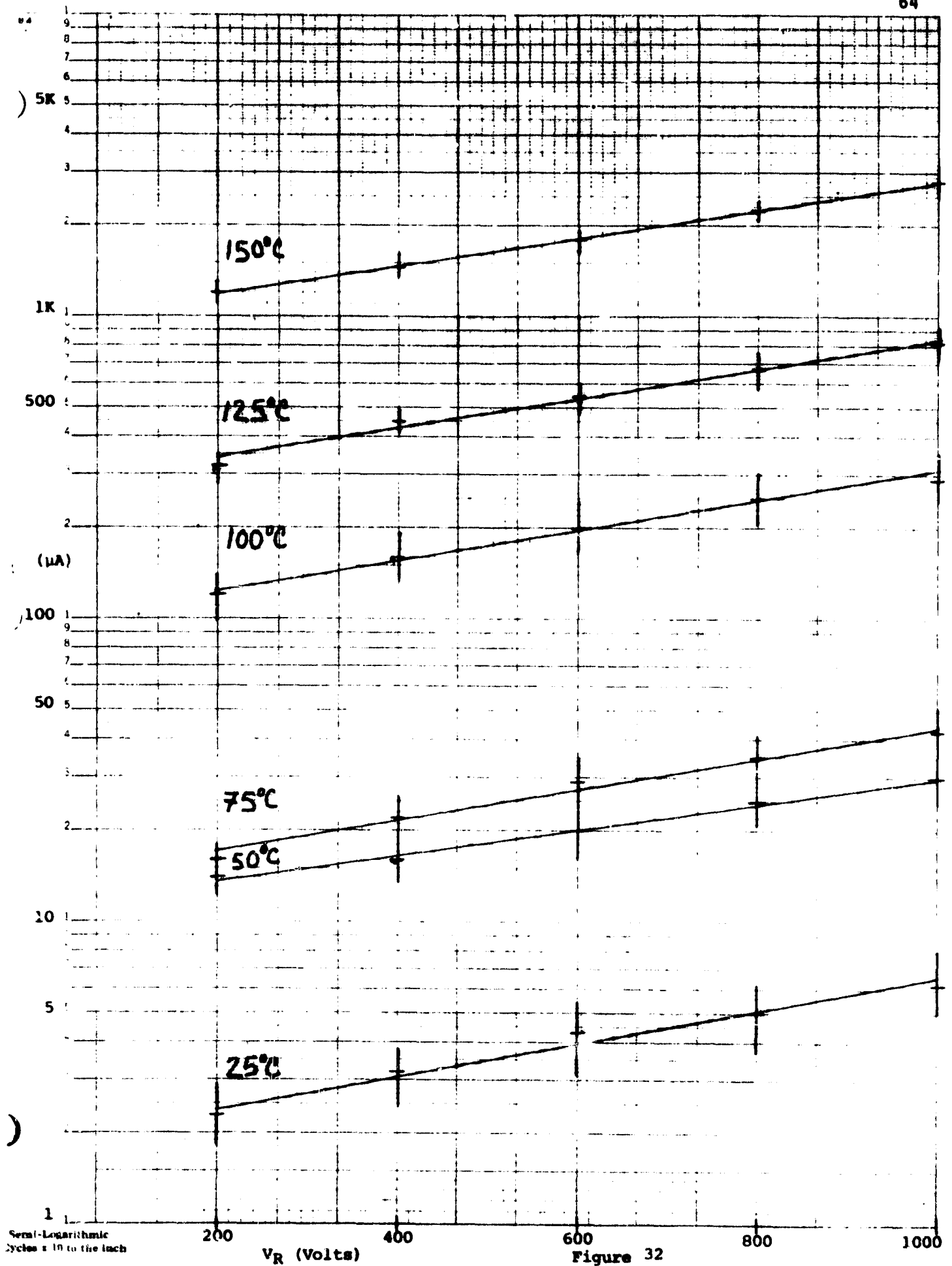


Figure 32

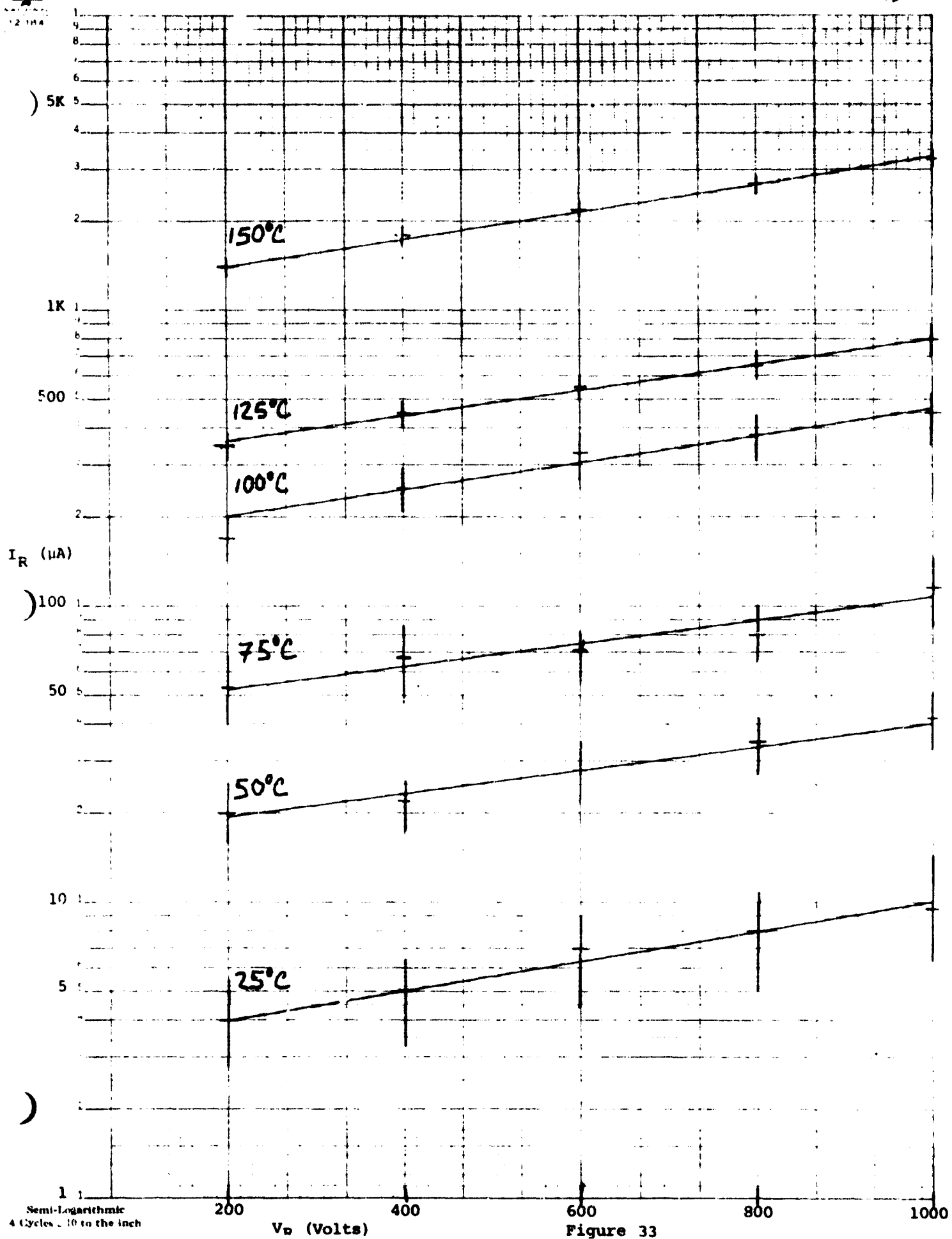
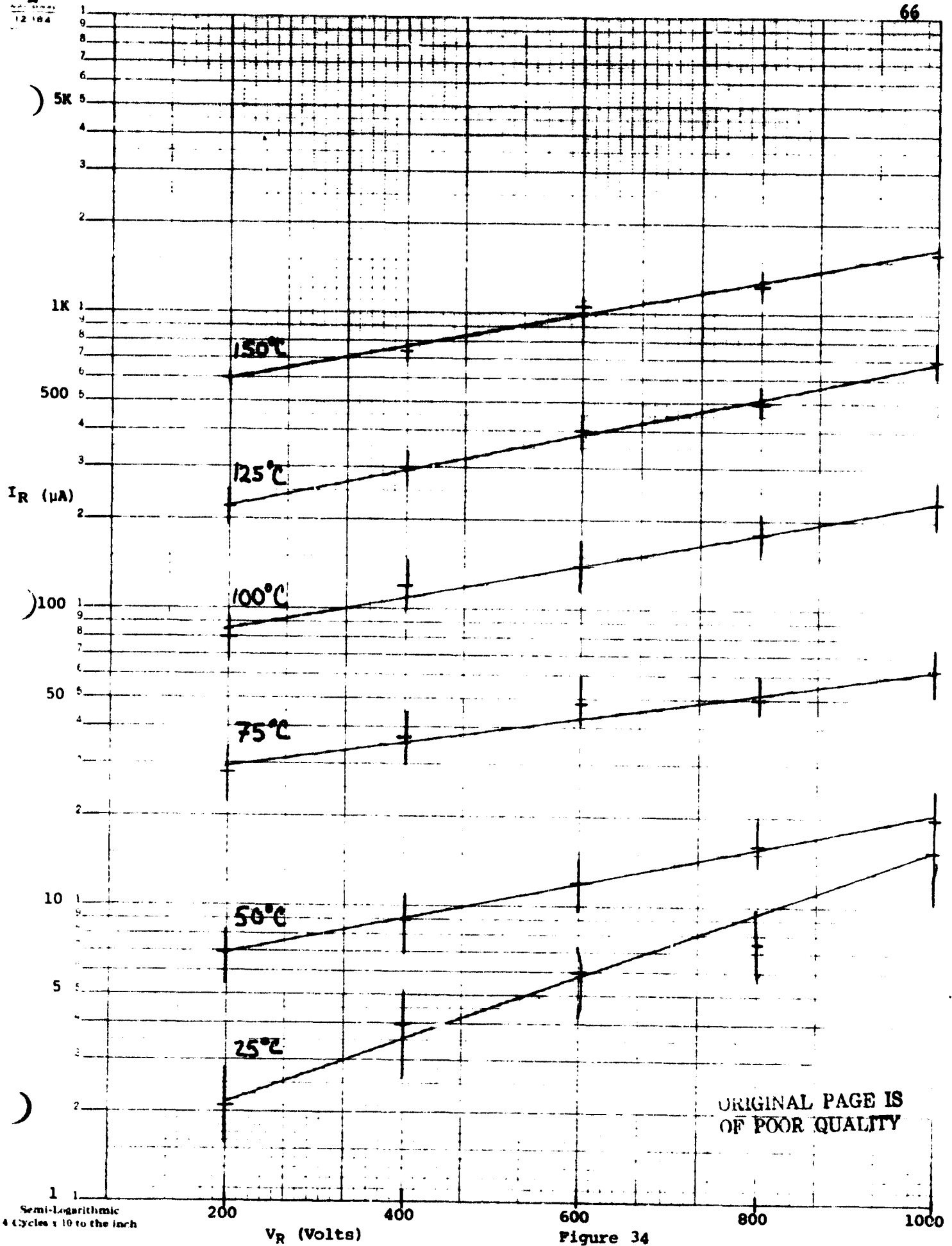


Figure 33



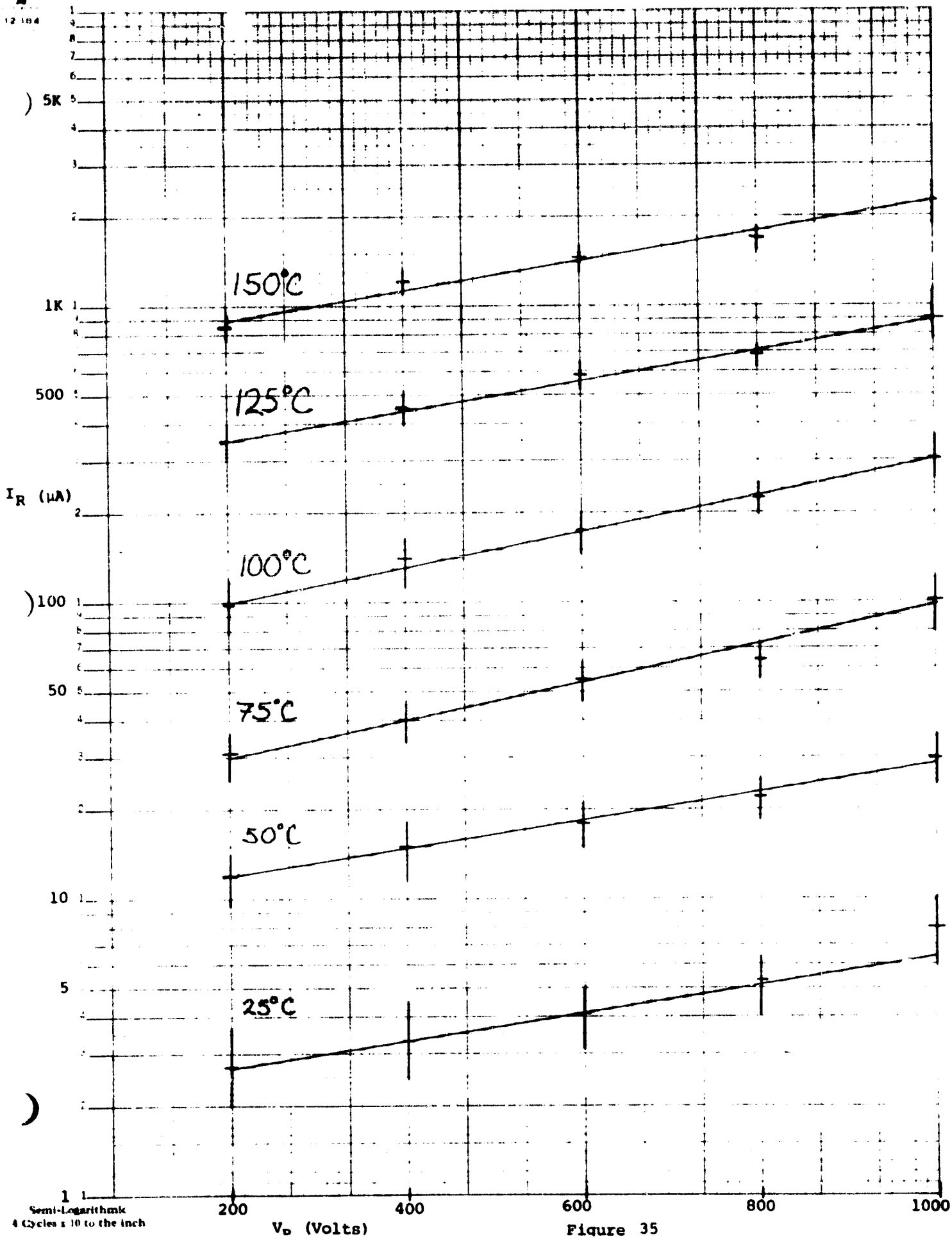


Figure 35

Leakage versus temperature

68

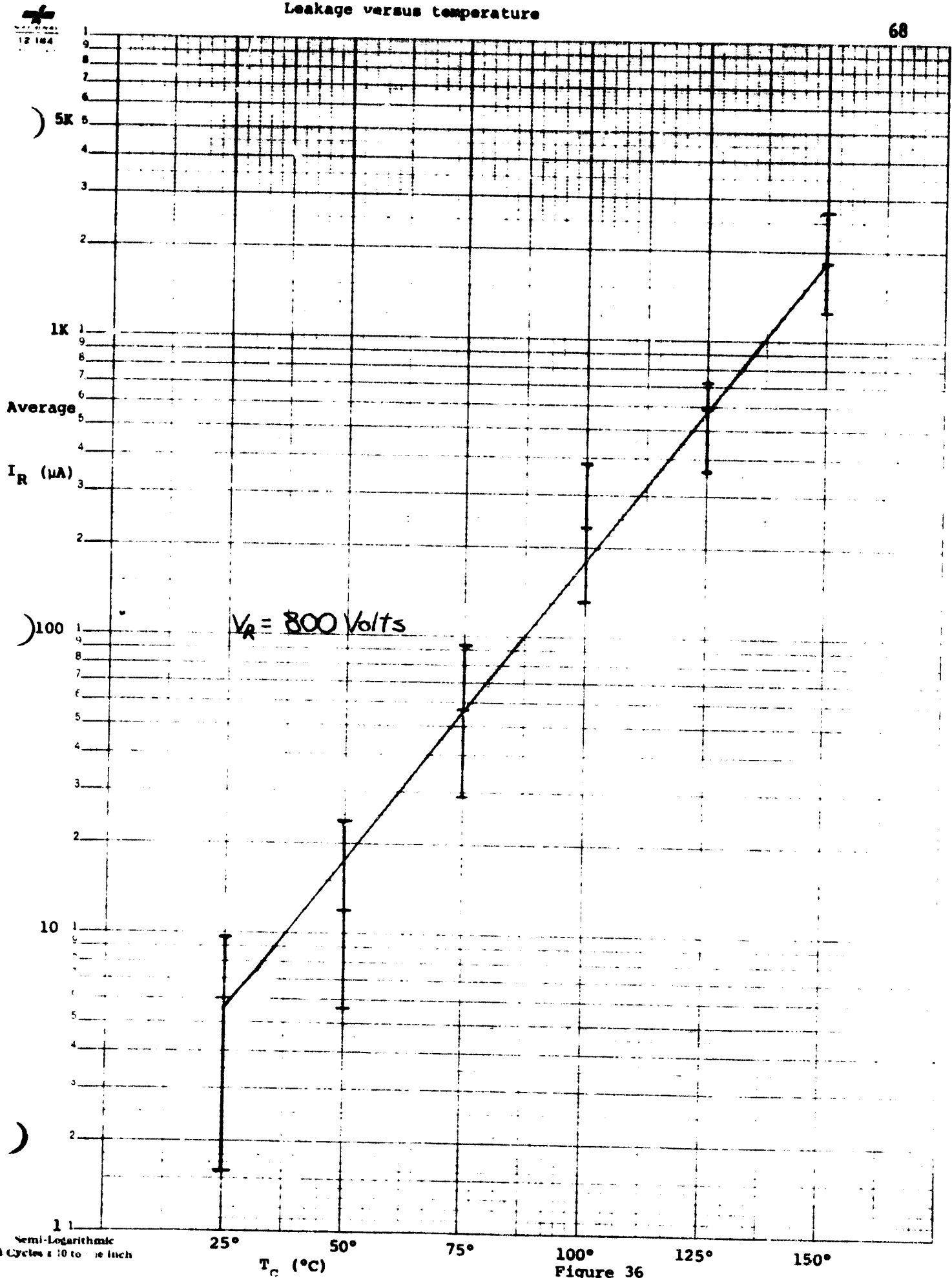


Figure 36

Device #031 Capacitance versus reverse voltage

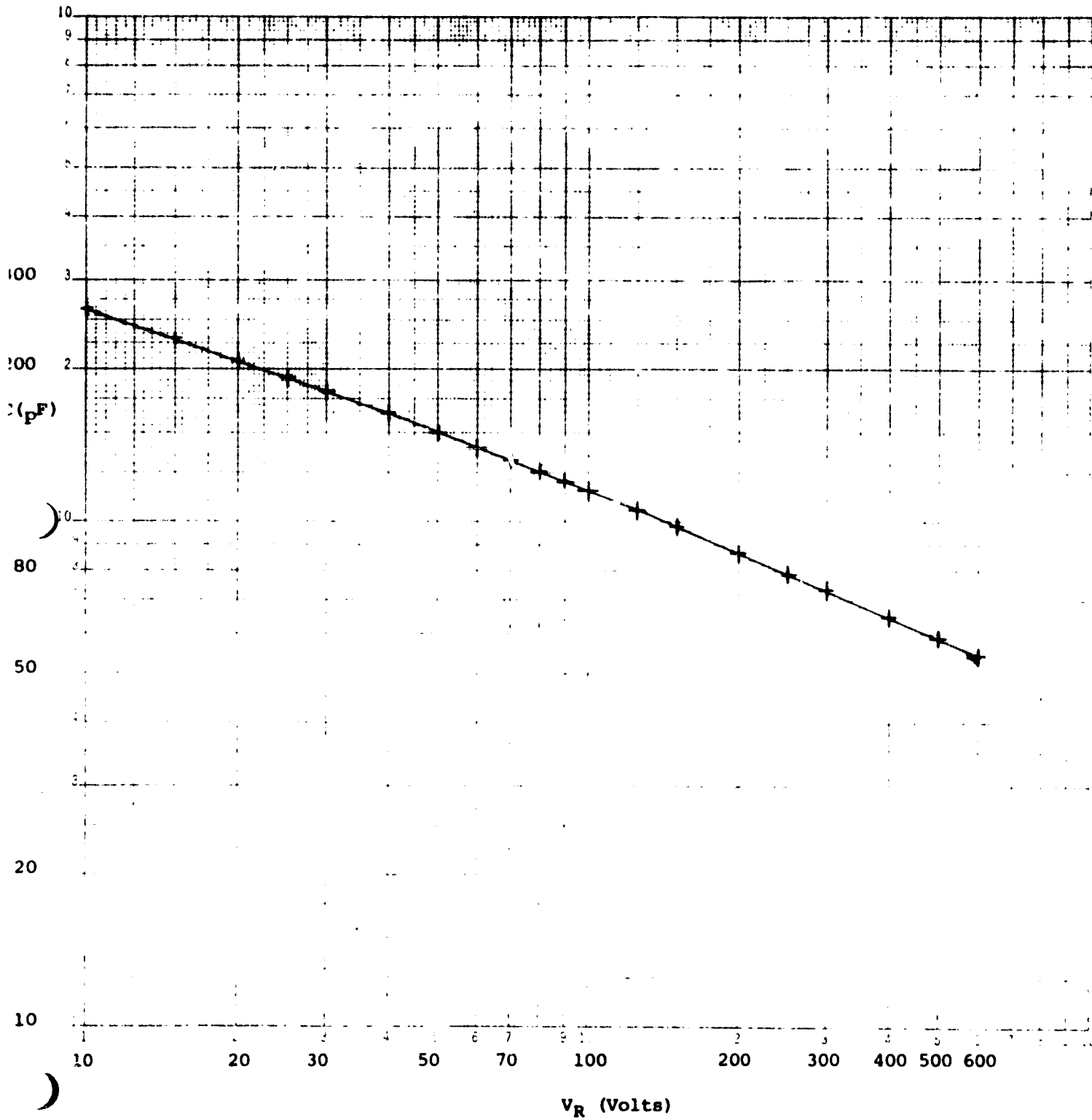


Figure 37



Device #038 Capacitance versus reverse voltage

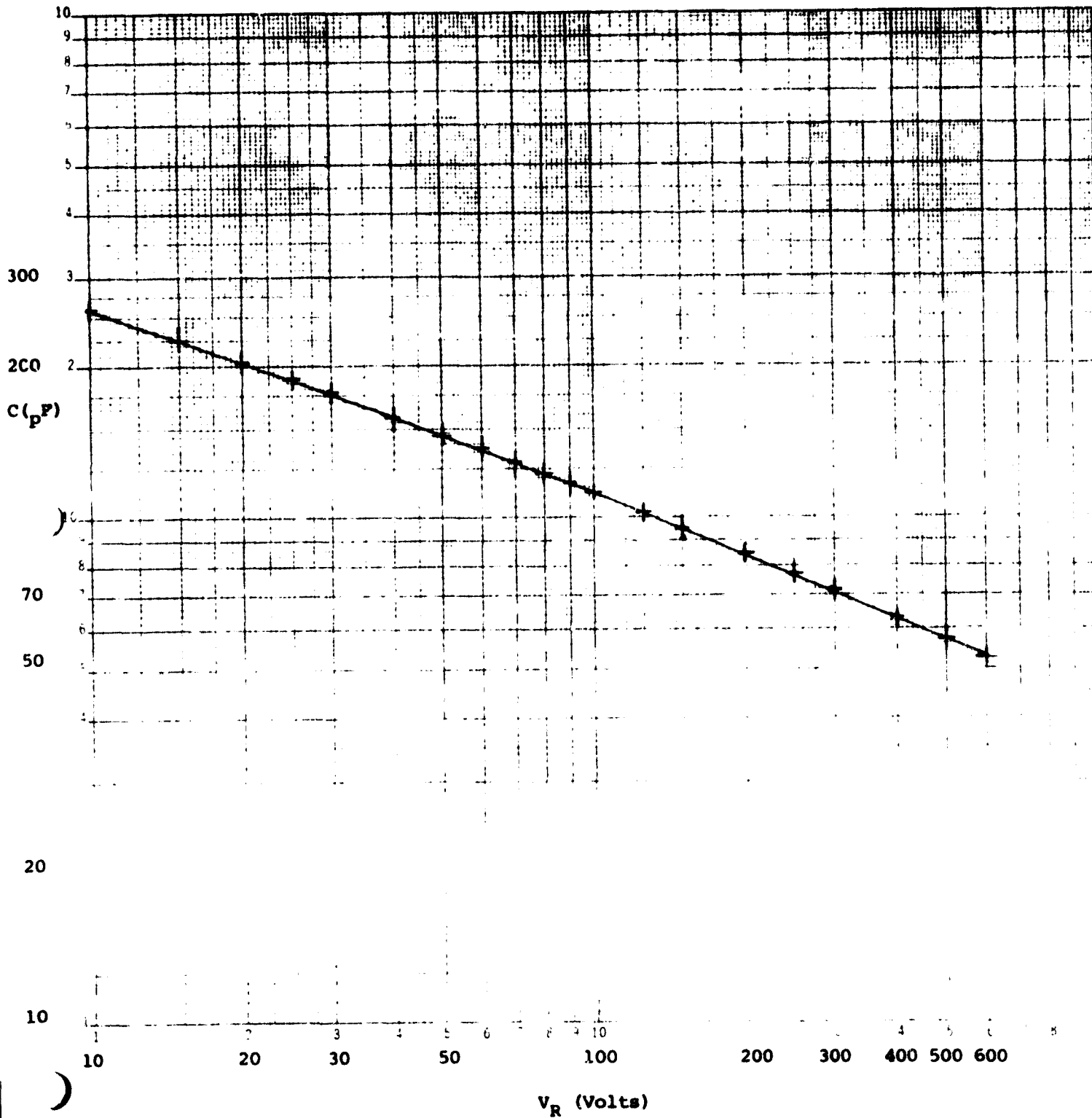


Figure 38



Device #039 Capacitance versus reverse voltage

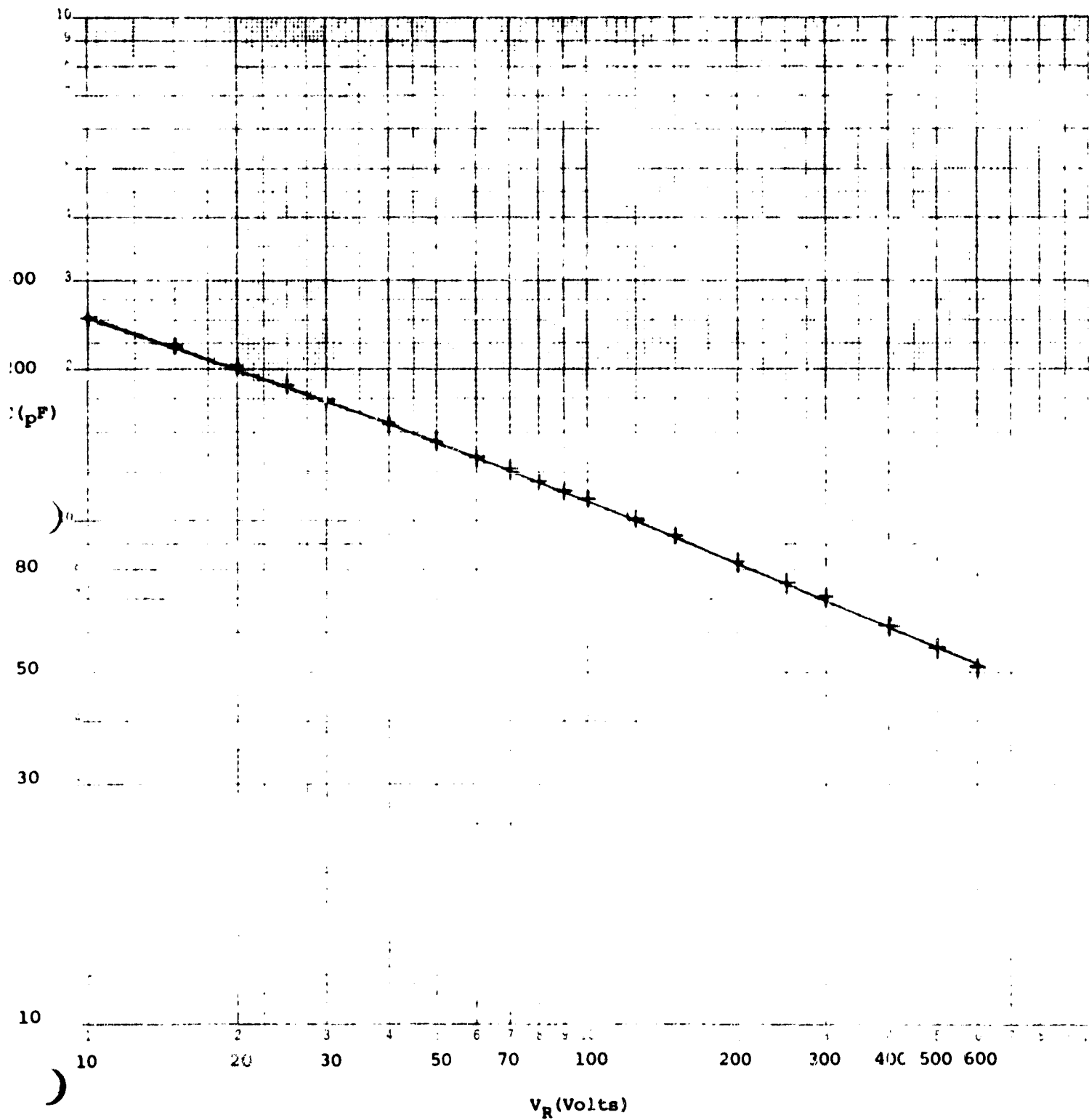
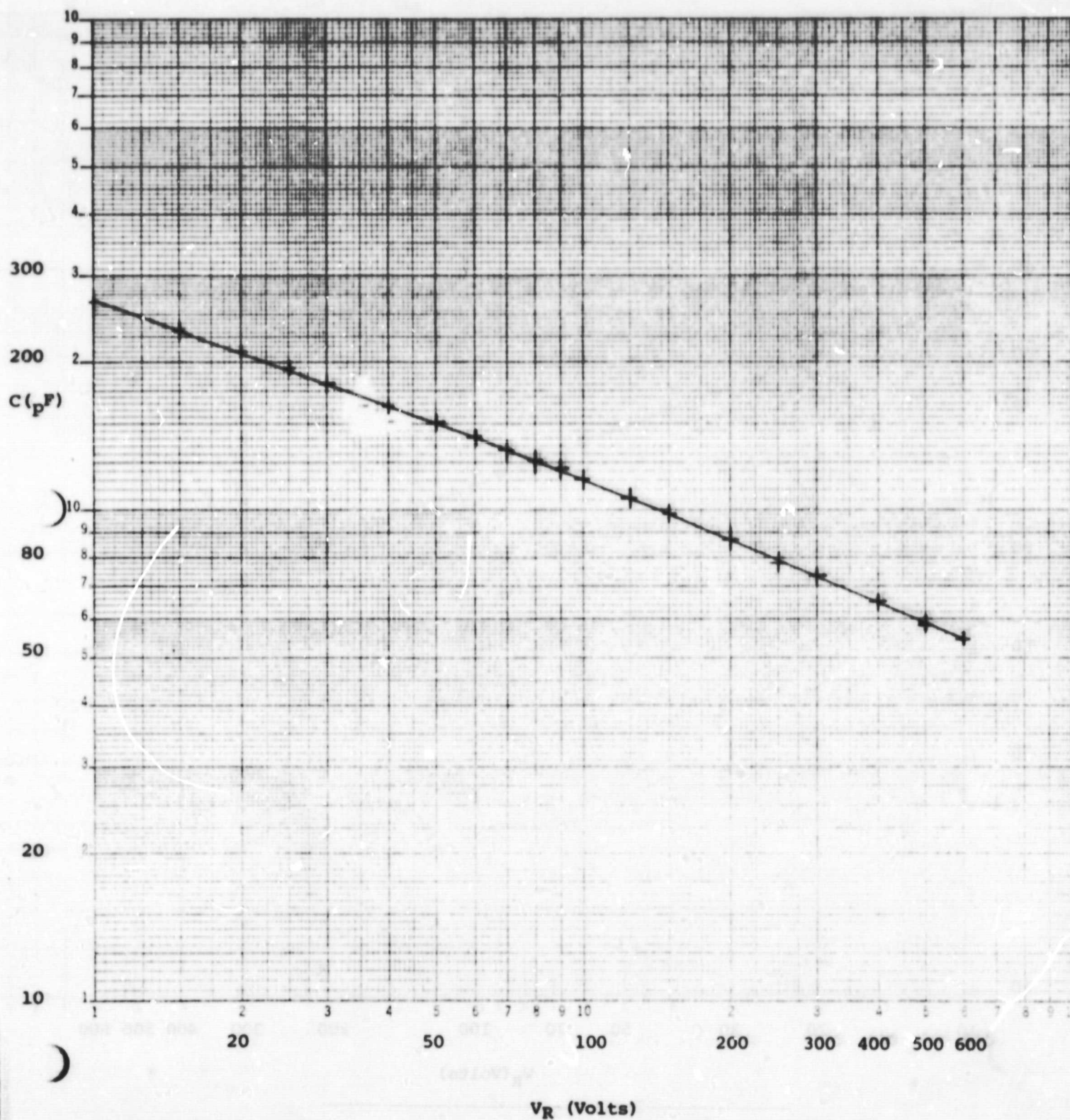


Figure 39

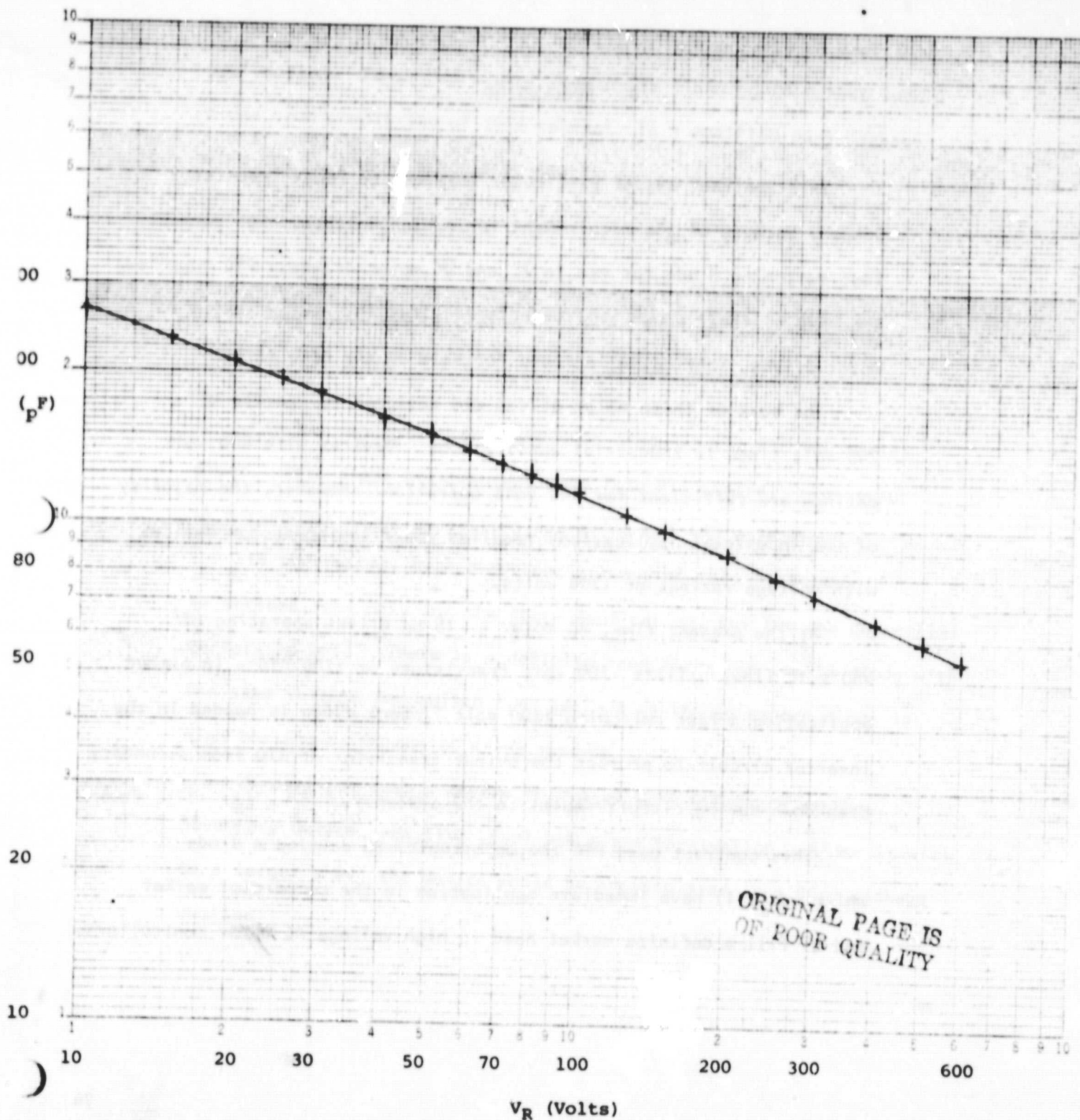
Device #046 Capacitance versus reverse voltage



V_R (Volts)

Figure 40

Device #060 Capacitance versus reverse voltage



ORIGINAL PAGE IS
OF POOR QUALITY

Figure 41

8. CONCLUSION

This contract was of particular interest to Power Transistor Company because of the requirement for a high voltage, high current, fast switching diode for use in AC and DC motor drives. PTC supplies the bulk of their power semiconductor devices for energy saving AC motor drives, fabricated in-house for sale on the open market.

The bulk of these motor drives are designed to operate off 240 volt lines in industrial applications. Devices with 600 volt ratings are sufficient for 240 volt operation. However, the majority of the industrial applications requires power semiconductor devices with voltage ratings of 1200 volts.

At the present time, AC motor 5 - 15 hp drives operating off 480 volt lines utilize 1200 volt transistors or 1200 GTO's in either application a fast switching 1200 volt flyback diode is needed in the inverter circuit to protect the output transistor or GTO from secondary breakdown during circuit faults in the system.

This contract gave PTC the opportunity to develop a diode which would 1) have immediate application in the commercial market and 2) fill a definite market need in high voltage AC motor controllers.

Currently, there are no diodes commercially available to meet this application. Power Transistor Company is planning to market such a diode upon completion of this contract, in a modified DO-5 package with the following specifications:

Peak inverse voltage	- 1200 volts minimum
Forward voltage @ 50 amperes	- 1.5 volts maximum
Reverse recovery time	- 400 nanoseconds maximum
Surge rating	- 600 amperes minimum

PTC has designated the 1200 volt diode as the PTC 900 series diode. This diode has been designed into PTC Controls prototype 15 horsepower AC drive systems operating off 480 volt lines.

In the future, higher current ratings of this diode should be pursued, not only for the space application, but for the commercial markets as well. There is a definite need for a 150 ampere diode with the same voltage and switch time ratings as the 50 ampere diode in high horsepower AC and DC drive systems.

We envision such a device to be the same structure as the 50 ampere device, positive bevel and glass passivation. Since it will be a larger area, the device would be encapsulated in a DO-9 package outline.

9. ACKNOWLEDGEMENTS

Editor: Vilnis Balodis

Contributors:

Albert H. Berman

James J. Duffin

Charles Gaugh

Helen M. Karatnicki

Guin Troutman

10. REFERENCES

1. A. H. Berman, "Avalanche Breakdown in Diffused P-N Junctions In Silicon", Private Communication (1980)
2. H. Lawrence and R. M. Warner, "Diffused Junction Depletion Layer Calculations", Bell Systems Tech. J. pg 47 (1959)
3. R. L. Davies and F. E. Gentry, "Control of Electric Field at the Surface of P-N Junctions", IEEE Transactions on Electron Devices, ED-11, No. 7, pg 313-323 (1964)
4. M. Otsuka, "The Forward Characteristics of Thyristors", Proceedings of the IEEE, Vol. 55, No. 1 pp. 1400-1408 (1967)

11.1 SPECIFICATIONS FOR FAST RECOVERY, HIGH VOLTAGE POWER DIODE CASE TEMPERATURE = 25°C UNLESS OTHERWISE SPECIFIED

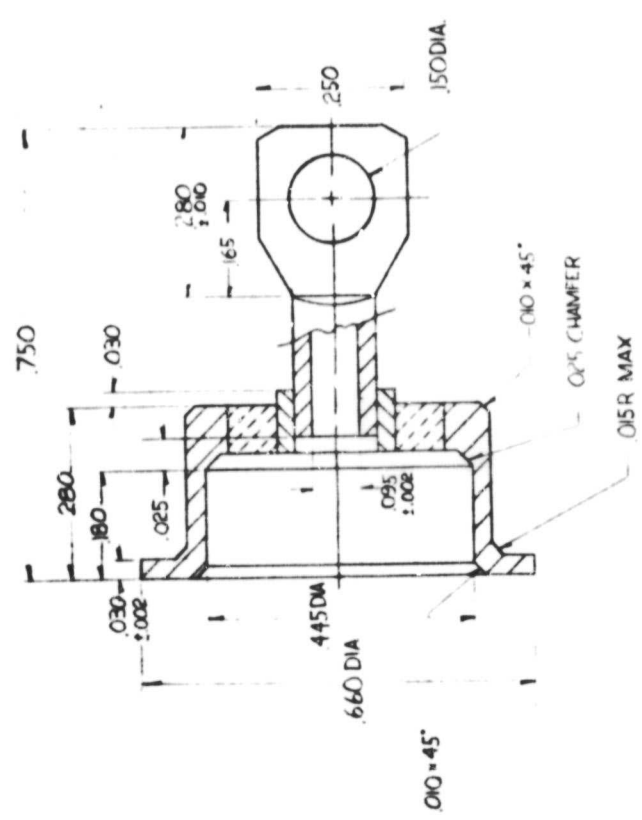
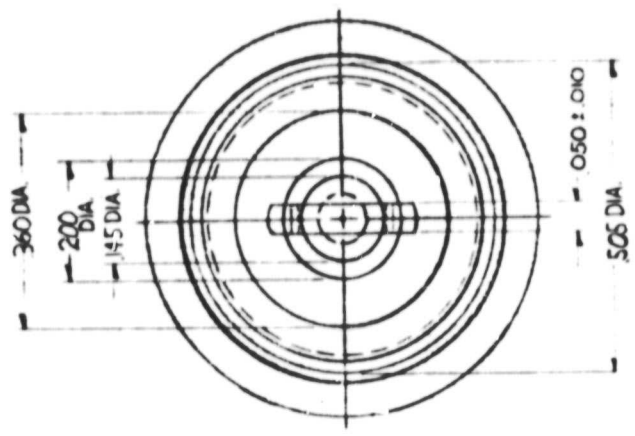
Type 1 - Fast Recovery Power Diode, 50A Avg. Current Rating

SYMBOL	CHARACTERISTICS WITH TEST CONDITIONS	VALUE	UNITS
V_{RRM}	Peak Repetitive Reverse Voltage, $T_J = 150^\circ\text{C}$	800 to 1000	Volts
V_R	DC Blocking Voltage, $T_J = 150^\circ\text{C}$	800 to 1000	Volts
V_{RSM}	Peak Non-repetitive Reverse Voltage, $T_J = 150^\circ\text{C}$	$\geq 1.25 V_{RRM}$	Volts
I_{RRM}	Max. Reverse Current at Rated V_{RRM} $I_F = 50\text{A}$ Forward Current $T_J = 25^\circ\text{C}$ $T_J = 150^\circ\text{C}$	0.05 5.0	Milliamps Milliamps
I_F	Average Forward Current at $T_C = 100^\circ\text{C}$	50	Amps
I_{FSM}	Non-Repetitive Peak Surge Current (1/2 cycle surge current at 60Hz under load)	1000	Amps
V_{FM}	Forward Voltage at Rated $I_F = 50\text{A}$	1.5	Volts
T_J	Operating Junction Temperature Range	-65 to 200	$^\circ\text{C}$
T_{STG}	Storage Temperature Range	-65 to 200	$^\circ\text{C}$
$R_{\theta JC}$	Thermal Resistance Junction to Case	0.5	$^\circ\text{C/W}$
t_{rr}	Reverse Recovery Time, $T_C = 100^\circ\text{C}$ $I_F = 1.0\text{A}$ to $V_R = 30 V_{dc}$ $I_{FM} = 50\text{A}$, $di/dt = 25\text{A}/\mu\text{sec}$ (JEDEC circuit)	50 200	nsec nsec
$I_{RM(REC)}$	Peak Reverse Recovery Current $I_{FM} = 50\text{A}$, $di/dt = 25\text{A}/\mu\text{sec}$ (JEDEC circuit)	5	Amps

ORIGINAL PAGE IS
OF POOR QUALITY

THE UNIVERSITY OF CHICAGO

REV	DATE	BY	DATE	APP'D
NC				



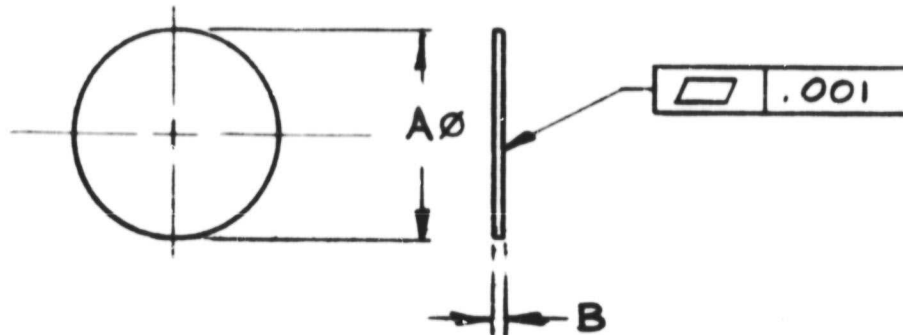
ITEM NO.	REV	DESCRIPTION	DATE	BY

PRECISION TRANSFORMER	
ANALOGUE, CALIF.	
TITLE	
DO-5 CAP HOUSING	
DATE	BY
5X	B
50-0016	NC

DESIGNED BY	CHECKED BY	APPROVED BY

NOTES: UNLESS OTHERWISE SPECIFIED

REVISIONS				
SYM	DESCRIPTION	BY	DATE	APPR'D



UNLESS OTHERWISE SPECIFIED		POWER TRANSISTOR CO. TORRANCE, CALIF., 90502			
TOLERANCES .XX ± _____ .XXX ± .002 ANGLES ± _____		SCALE: NONE	APPROVED BY <i>[Signature]</i>	CHECKED BY <i>[Signature]</i>	DRAWN BY <i>[Signature]</i>
		DATE: 25 APR 80	SHEET 1 OF 2		
		TITLE MOLY TAB, ROUND			
				REV N/C	DRAWING NUMBER 50-0003

DWG NO.	DIM. A	DIM. B	MATERIAL	FINISH	
-1	.160	.010/.012	1	2	
-2	.300	.010/.012	1	2	
-3	.310	.010/.012	1	2	
-4	.250	.010/.012	1	2	

ORIGINAL PAGE IS
OF POOR QUALITY

3. REMOVE BURRS.

2. FINISH: NICKEL PLATE

1. MATERIAL: MOLYBDENUM

NOTES: UNLESS OTHERWISE SPECIFIED

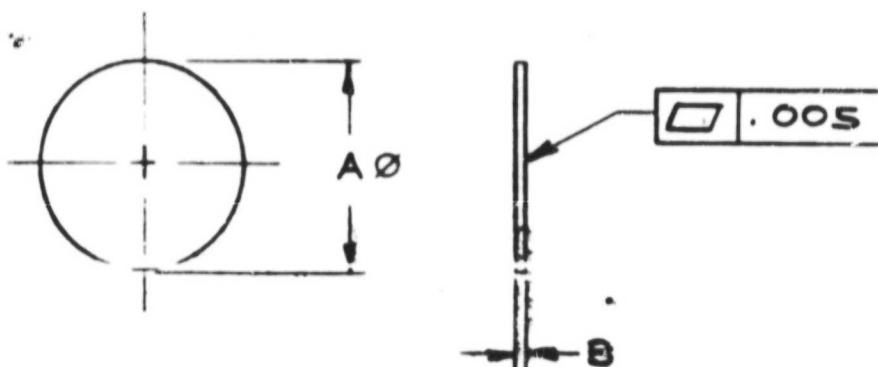
SCALE NONE	DWG NO.	REV
SHEET 2 OF 2	50-0003	N/C



- NOTES: UNLESS OTHERWISE SPECIFIED

[illegible]

REVISIONS				
SYN	DESCRIPTION	BY	DATE	APPR'D
A	ADD DIMS NO -5	V.B.	10/10/80	<i>[Signature]</i>



UNLESS OTHERWISE SPECIFIED	POWER TRANSISTOR CO. TORRANCE, CALIF., 90502			
TOLERANCES .XX ± _____ .XXX ± .002 ANGLES ± _____	SCALE: NONE	APPROVED BY <i>[Signature]</i>	CHECKED BY <i>[Signature]</i>	DRAWN BY <i>[Signature]</i>
	DATE: 25 APR 80	SHEET 1 OF 2		
	TITLE PREFORM, SOLDER, ROUND			
	REV A			DRAWING NUMBER 50-0004

DWG NO.	DIM. A	DIM. B	MATERIAL
-1	.150	.002/.003	1
-2	.300	.002/.003	1
-3	.160	.002/.003	2
-4	.310	.002/.003	2
-5	.160	.002/.003	3
-6	.250	.002/.003	3
-7	.160	.002/.003	3

ORIGINAL PAGE IS
OF POOR QUALITY

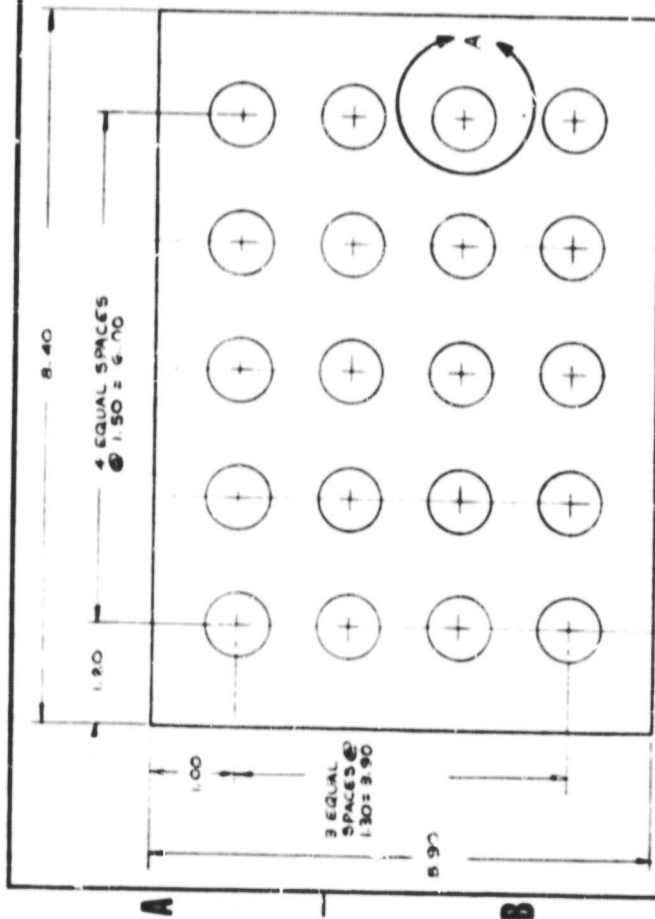
3 MATERIAL: SOLDER 50/50 Pb/In

2 MATERIAL: SOLDER 92.5/2.5/5.0, Pb/Ag/In

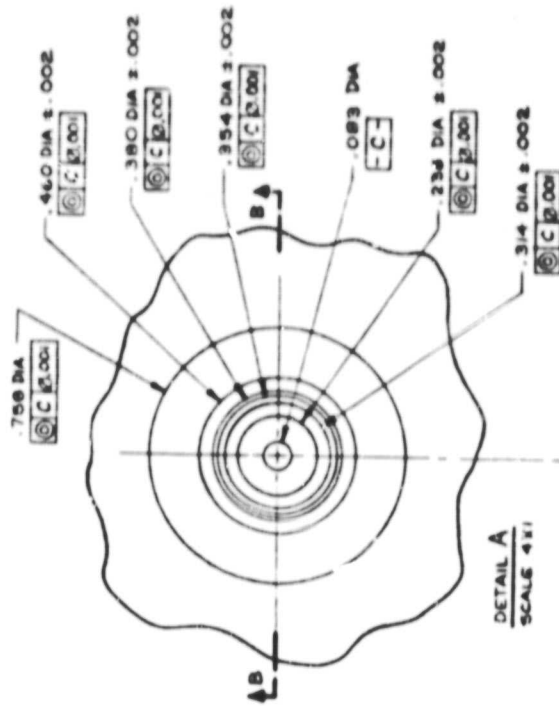
1 MATERIAL: SOLDER 5/95, Sn/Pb.

NOTES: UNLESS OTHERWISE SPECIFIED:

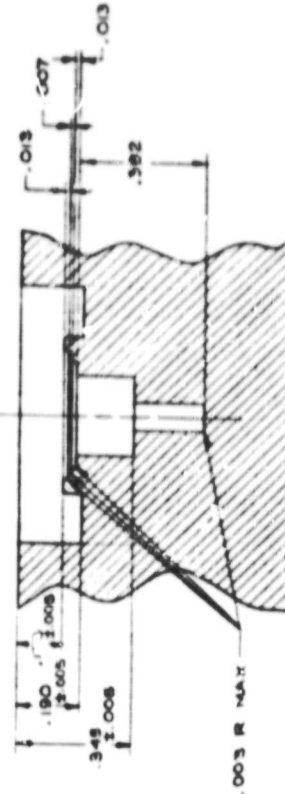
SCALE NONF	DWG NO.	REV
SHEET 2 OF 2	50-0004	A



ORIGINAL PAGE IS
OF POOR QUALITY



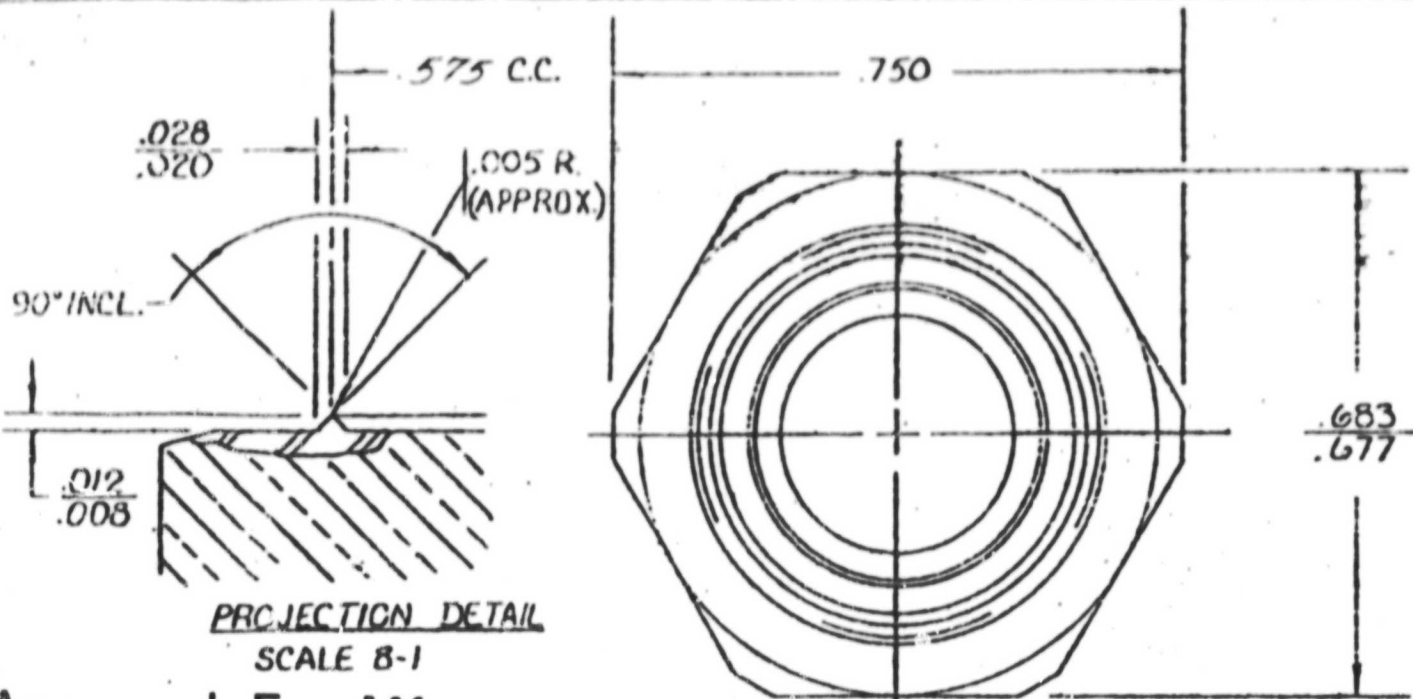
DETAIL A
SCALE 4X1



SECTION B-B
SCALE 4X1

POWER TRANSLATOR CO. TORRANCE, CA.		C 50-0010	
FIXTURE, SOLDERING		C 50-0010	
NASA		FULL	
DATE		DATE	
BY		BY	
CHECKED		CHECKED	
APPROVED		APPROVED	

3. REMOVE BURRS.
 2. ALL DIMENSIONS ARE IN INCHES.
 1. MATERIAL: GRAPHITE, SPBR KK-10 OR EQUIV.
- NOTES: UNLESS OTHERWISE SPECIFIED



Approved For Mfg.

UNLESS OTHERWISE SPECIFIED
.005 BRK
.005 MAX. DEPTH
.450 MAX. Ø GROOVE

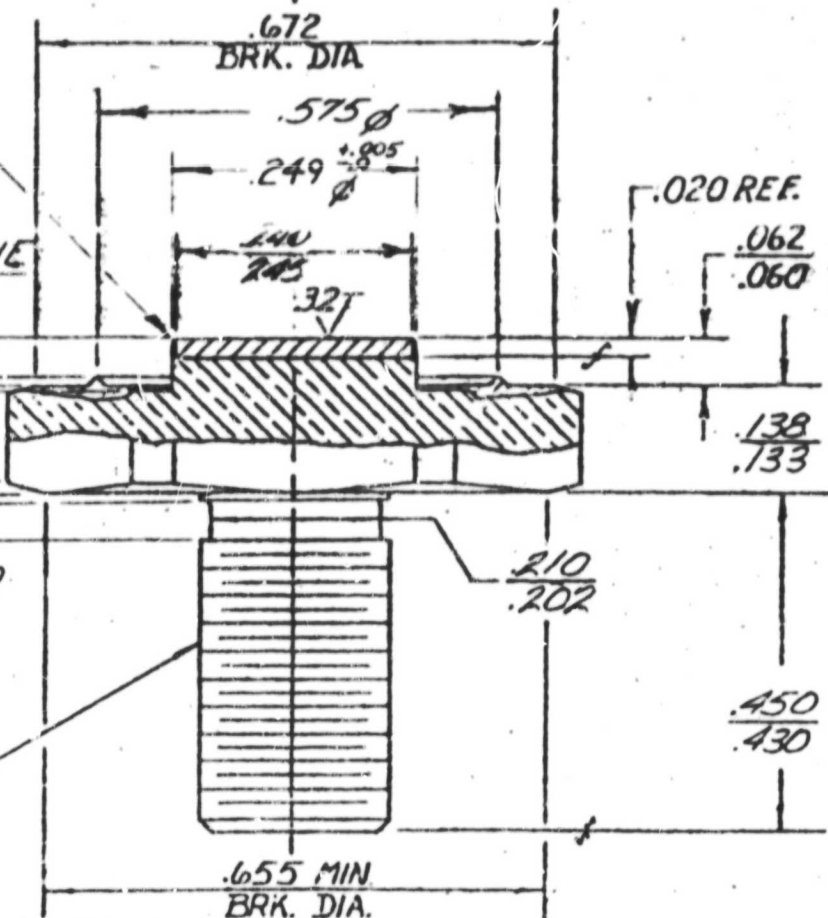
11 A .002
□ .001

11 A .002
□ .001

A □ .001

15° TYP.

.005 MAX
(BEFORE PLATING)
1/4-28 UNF-2A (MOD)
PITCH DIA
MAX. 2240 MIN. 2225
MAJOR DIA.
MAX. 2472 MIN. 2425



THE *Nippst* COMPANY

633 PITTSBURGH DR.



DELAWARE, O.

TOLERANCES UNLESS OTHERWISE SPECIFIED

FRACTIONS ± .010

DECIMALS ± .005

ANGLES ± 2°

5° MACH'D SURF.

ORIGINAL PAGE IS
OF POOR QUALITY

APPROVED BY SS

DATE 7-27-78

DRAWN BY Kot

DATE 7-29-78

© "N.A." — REGISTERED TRADEMARK
APPLICABLE U.S. AND FOREIGN PATENTS LISTED
ON SHIPPING CARTONS. OTHER PATENTS PENDING.

MATERIAL
NOTED

PART NAME
STUD BASE

SHEET

ISSUED

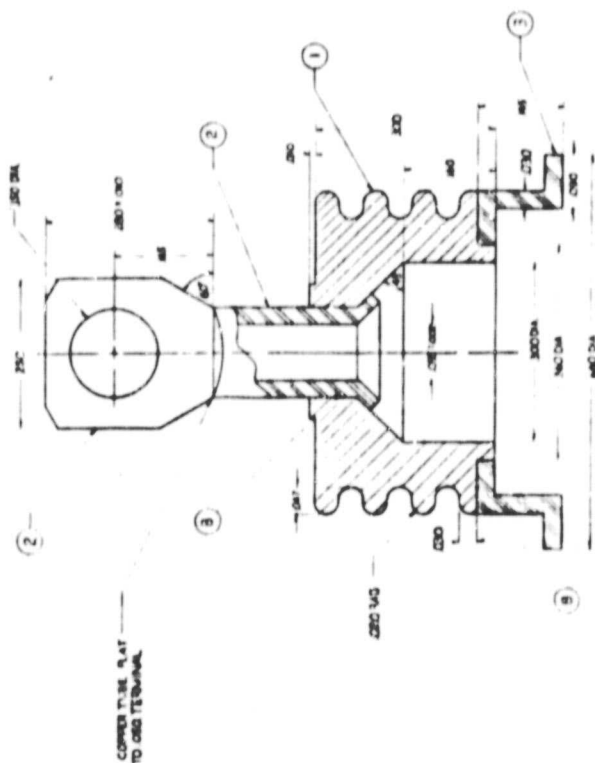
FEB 18 1980

SCALE 4=1

PART NO. 068-8923

REV 05

Technical drawing of a mechanical assembly, likely a pump or valve, showing a cross-section of a cylindrical body with internal components and a flange. The drawing includes dimension lines and labels in Chinese characters.

[illegible]